Distribution Agreement

In presenting this thesis as a partial fulfillment of the requirements for a degree from Emory University, I hereby grant to Emory University and its agents the non-exclusive license to archive, make accessible, and display my thesis in whole or in part in all forms of media, now or hereafter now, including display on the World Wide Web. I understand that I may select some access restrictions as part of the online submission of this thesis. I retain all ownership rights to the copyright of the thesis. I also retain the right to use in future works (such as articles or books) all or part of this thesis.

Celia Bianco March 25, 2024

Age-Dependent Roles of C1q in Ia Afferent Synapse Dynamics Post-Peripheral Nerve Injury: A Comparative Study in Neonates and Adults

by

Celia Bianco

Francisco J. Alvarez, Ph.D.
Adviser

Neuroscience and Behavioral Biology

Francisco J. Alvarez, Ph.D.

Adviser

Jill Ward, Ph.D.

Committee Member

Keith Easterling, Ph.D.

Committee Member

2024

Age-Dependent Roles of C1q in Ia Afferent Synapse Dynamics Post-Peripheral Nerve Injury: A Comparative Study in Neonates and Adults

By

Celia Bianco

Francisco J. Alvarez, Ph.D.

Adviser

An abstract of
a thesis submitted to the Faculty of Emory College of Arts and Sciences
of Emory University in partial fulfillment
of the requirements of the degree of
Bachelor of Science with Honors

Neuroscience and Behavioral Biology

2024

Abstract

Age-Dependent Roles of C1q in Ia Afferent Synapse Dynamics Post-Peripheral Nerve Injury: A Comparative Study in Neonates and Adults

By Celia Bianco

Peripheral nerve injuries, especially those involving nerve transections, frequently cause reduced functionality. These injuries lead to the irreversible loss of Ia proprioceptive synapses from their target motoneurons, preventing full functional recovery despite nerve regeneration and muscle reinnervation. Consequently, the monosynaptic muscle stretch reflex disappears, leading to impaired fine motor control in affected individuals. Crush injuries, however, do not cause this permanent loss of Ia afferent synapses, and therefore, the muscle stretch reflex returns. The recovery pattern after crush injuries shifts dramatically during the early postnatal period, a crucial phase for developing weight-bearing movements. Injuries inflicted at this stage result in far greater and more permanent Ia afferent synaptic losses than when this injury occurs during adulthood. Notably, the extent of Ia afferent synaptic loss from neonatal crush injuries closely mirrors that of full nerve transections in adults. These permanent synaptic losses occur despite successful muscle reinnervation and no evidence of peripheral immune cell invasion, which has been implicated in removing these contacts after nerve transections in adults. This early developmental window is marked by an upregulation of complement proteins by microglia, triggering the complement cascade for developmental synaptic pruning to refine motor circuits. Considering the pivotal role of C1q, the complement cascade's initiating protein, in synaptic pruning during both development and pathology, our study investigates C1q's involvement in post-injury synaptic pruning and its differential impact between neonates and adults. We examined two cohorts: neonates subjected to sciatic nerve crush injuries, with and without global C1q deletion, and adults undergoing sciatic nerve transection, including animals with C1q selectively removed from microglia prior to injury, and their genetic control littermates. Our analysis on the quantity of VGLUT1 synaptic boutons on injured motoneurons reveals a stark contrast; unlike in adults, where synaptic contacts decrease after nerve transection regardless of C1q presence, VGLUT1 contacts in neonates are preserved in the absence of C1q. However, these synapses are significantly reduced in size, indicating diminished functionality. This finding emphasizes C1q's distinct role in synaptic pruning following nerve injuries across developmental stages and suggests an age-dependent mechanism of synaptic loss post-injury. It provides new insights into the complex interplay between injury, development, and synaptic plasticity.

Age-Dependent Roles of C1q in Ia Afferent Synapse Dynamics Post-Peripheral Nerve Injury: A Comparative Study in Neonates and Adults

By

Celia Bianco

Francisco J. Alvarez, Ph.D.

Adviser

A thesis submitted to the Faculty of Emory College of Arts and Sciences
of Emory University in partial fulfillment
of the requirements of the degree of
Bachelor of Arts with Honors

Neuroscience and Behavioral Biology

2024

Acknowledgements

I would like to thank the Mentis Lab for their collaboration on this project and for generously providing most of the mice needed for this research. Special thanks go to Danny Florez-Paz for performing animal husbandry, surgeries, and tissue dissections.

I'm grateful to my committee members for their valuable feedback and guidance, which helped improve this project and kept my goals achievable.

I would like to thank my family for their constant support and encouragement, even from over 1,000 miles away. A special shoutout to my mom, who has always been my first audience member while I am practicing for any of my presentations.

I must also extend my sincere thanks to my friends, particularly Shannon Zhang, Katelyn King, Brian Graham, Darin Kishore, Veronica Amores-Sanchez, Pono Wong, Elise Boudreau, and the entire Raoul Hall staff. From keeping me company during long nights at the confocal microscope to forcing me to take breaks when I am feeling stressed, you all have kept me sane and motivated throughout my time here at Emory.

I'd like to express my gratitude to Tana Pottorf, Elizabeth Lane, Will McCallum, Andrew Worthy, Olivia Mistretta, Dr. Paula Martin Calvo, and Dr. Ron Griffith for being incredible role models and friends in the lab. More than just being people I look forward to seeing every day, they have significantly contributed to my understanding of our research. I'm thankful for the opportunities to observe various procedures and for their eagerness to share their help and expertise.

I am incredibly grateful to Dr. Alvarez for the opportunity to work on this project under his mentorship. He always made sure I understood not just what I was doing, but also why it was important. I also thank him for his dedication to editing this manuscript, even over weekends, ensuring the final product is something we can all be proud of.

Finally, thank you to Zoë Haley-Johnson for her invaluable contributions that are too many to list. Zoë has taught me all the techniques I used in this project, given me detailed feedback, and supported me every step of the way. Whether it was opening the lab on weekends or encouraging me after a tough presentation, Zoë has gone above and beyond to make sure I succeed and enjoy my time in the lab. This project simply wouldn't have been possible without her.

Table of Contents

INTRODUCTION

Epidemiology of Peripheral Nerve Injury

Peripheral nerve injury (PNI) is a condition characterized by the disturbance or damage to the peripheral nervous system (PNS), a complex network of nerves that connects various body parts to the central nervous system (CNS). It impairs the normal function of the peripheral nerves, leading to problems in transmitting signals between the CNS and the muscles, skin, and internal organs (Lopes et al., 2022). This condition often results in significant functional deficits, such as loss of sensory and motor abilities, muscle atrophy, chronic pain, and weakness (Zhang et al., 2022). Between 13 and 23 out of every 100,000 people are affected by PNI, and approximately 90% of those who suffer from PNI do not attain complete motor or sensory recovery (Dong et al., 2021; Portincasa et al., 2007; Scholz et al., 2009).

Peripheral nerve injuries impact individuals of all ages, yet the prevalence of specific types of these injuries tends to shift with age. In adults, ulnar nerve injuries, often resulting from motor vehicle crashes, are among the most common PNIs (Althagafi and Nadi, 2023). Despite axonal regeneration and muscle reinnervation, about 90% of patients continue to experience impairments years after injury (Portincasa et al., 2007). Ulnar nerve injuries impair fine motor skills, particularly affecting the ability to pinch, hold objects like pens, and button shirts due to muscle weakness or paralysis. This results in reduced coordination and dexterity, complicating precise hand movements (Lleva et al., 2023).

In children, the brachial plexus is the nerve network most commonly affected. This network is crucial for sensation and muscle control in the shoulder, arm, hand, and fingers

(Govindan and Burrows, 2019). Brachial plexus injuries usually occur from stretch injuries to the head, neck, and shoulder, often during birth. The incidence of these injuries ranges between 0.4 to 4 per 1,000 live births (Govindan and Burrows, 2019). While the severity of the injury greatly influences recovery, approximately 20-30% of children with brachial plexus injuries are left with residual deficits (Volpe et al., 2018). Given the prevalence of PNIs and the low likelihood of complete recovery for those affected, it becomes increasingly important to deepen our understanding of the underlying mechanisms involved in both the injury itself and the subsequent regeneration.

Degenerative Processes Following Peripheral Nerve Damage

Following a peripheral nerve injury, cellular and molecular mechanisms are activated first at the site of injury in the periphery. These mechanisms orchestrate a series of events tailored to the specific nature of the injury, guiding either the degeneration or the potential regeneration of the affected nerve fibers. Peripheral nerve injuries are classified into three main types: neuropraxia, axonotmesis, and neurotmesis (Sunderland, 1951). Neuropraxia, the mildest form, arises from mild compression of the nerve, leading to a temporary disruption in nerve function (Menorca et al., 2015). This condition is characterized by decreased conduction velocity due to focal segmental demyelination, yet it preserves axonal continuity without any loss of the axon itself. In contrast, axonotmesis, otherwise known as a “crush” injury, involves the severance of axons while preserving the connective tissue sheaths around them (Menorca et al., 2015). Neurotmesis, also referred to as "cut" injuries, represents the most severe form of nerve damage. This type involves the complete severance of the nerve fibers (axons) as well as the

surrounding connective tissues, disrupting both the electrical signaling and the structural integrity of the nerve (Menorca et al., 2015).

Following axonotmesis and neurotmesis, the severed nerve undergoes a degenerative process known as Wallerian degeneration, whereby the nerve breaks down to help establish a microenvironment that facilitates axonal regeneration (Menorca et al., 2015). Despite not having experienced the trauma directly, the distal segments of the injured axons deteriorate due to their severed connection from the neuron's cell body, thereby losing access to essential nutrients and metabolic support (Rotshenker, 2011). The speed of this process is proportional to the pace of regeneration, with faster degeneration leading to a quicker and usually more successful recovery (Rotshenker, 2011). The proximal stump also degenerates but is much less severe as it typically only progresses to the first node of Ranvier. When the injury site is close to the neuronal cell body in the dorsal root ganglion (DRG), however, apoptosis may occur, thus eliminating the potential for axon regeneration (Tetzlaff and Bisby, 1989).

The first step in Wallerian degeneration is axon fragmentation. The rate of this process is dependent on several factors, including the diameter of the axon, the distance between the injury and the end-organ, and the species experiencing the injury (Lubińska, 1977; Beirowski et al., 2005; Gilliatt and Hjorth, 1972). Generally, injured axons with a smaller diameter, shorter distal segments, and belonging to smaller-sized animals tend to fragment more quickly. Fragmentation can be observed through light microscopy within 36 to 44 hours post-nerve transection in rodents, whereas in baboons, it is only detectable about one week after the injury (Lubińska, 1977; Gilliatt and Hjorth, 1972). Furthermore, large, heavily myelinated afferent fibers, such as the proprioceptive Ia afferents that transmit information regarding muscle length and dynamics,

undergo degeneration and subsequent regeneration more slowly compared to afferent fibers with less myelin and a smaller diameter, such as the Ib fibers, which play a crucial role in touch sensation. Following fragmentation, axon destruction progresses from the site of injury towards the muscle, advancing at a rate of about 10 to 24 millimeters per hour (Rotshenker, 2011).

These afferent fibers not only disconnect from their innervated muscles, but they also disconnect from their contacts upon neurons in the spinal cord. When sensory axons are injured, they disconnect form target muscles and also withdraw their connections with neurons in the spinal cord (Blinzinger and Kreutzberg, 1968). This prevents motor neurons from receiving sensory input (Alvarez at al., 2010; Alvarez et al., 2011). The severity of synaptic stripping differs between axonotmesis and neurotmesis injuries, with both involving activated microglia surrounding motor neurons, but only after neurotmesis injuries the microglia reaction extend in time causing a phenotypic change in activated microglia towards expression of the chemokine C-C motif ligand 2 (CCL2) and infiltration of C-C motif receptors (CCR2) positive blood-borne immune cells responding to this chemokine (Rotterman et al., 2024). The extent of this immune reaction and CCL2-CCR2 signaling determines whether synapses from muscle sensory afferents return to their target neurons.

Ia sensory afferents are nerve fibers that play a critical role in the body's proprioceptive system, primarily by innervating muscle spindles in the periphery. These muscle spindles are sensory receptors located within the muscle that detect changes in muscle length, effectively providing the central nervous system with information about the position and movement of limbs. Upon detecting a stretch in the muscle, Ia afferents transmit signals to motorneurons in the spinal cord, triggering the stretch reflex. This reflex involves the immediate contraction of the

stretched muscle and relaxation of the antagonist muscle, thereby preventing overstretching and injury. The disappearance or dysfunction of Ia afferents disrupts this feedback loop, leading to deficits in motor control. Without the precise input from muscle spindles via Ia afferents, the central nervous system struggles to accurately gauge muscle position and movement, resulting in impaired coordination and difficulty executing fine movements, such as those involved during slope walking (Maas et al., 2007). This is because balance and adjustments required for such fine motor tasks rely on the instantaneous feedback provided by these sensory afferents.

Peripheral Nerve Regeneration

Once Wallerian degeneration is complete in the peripheral nerve, regeneration begins (Dahlin, 2006). The remaining part of the nerve closest to the body is known as the proximal stump and it is connected to the cell body that resides in dorsal root ganglia (DRGs). Transected axons start growing by making many different sprouts. Many of these branches are pruned, leaving the survivors to continue growing (Morris et al., 1972). The growth of these axons relies on structural proteins produced both locally and within the cell body, which are then anterogradely transported along the axon. These proteins include actin and tubulin (Fu and Gordon, 1997; Ertürk et al., 2007; McQuarrie, 1985). Because these building materials travel slowly, axon regeneration progresses at a rate of 1-3 mm per day (Griffin et al., 2013). At the forefront of each growing axon is a structure known as a growth cone. This cone guides the axon toward the far end of the nerve, the distal stump, by reacting to environmental guidance signals known as neurotrophins. Depending on the signals, growth cones can be drawn towards or

pushed away from specific areas, ensuring the axons grow in the correct direction to ultimately reconnect to their targets (Goodman, 1996; Tuttle and O'Leary, 1998).

Schwann cells play crucial roles in nerve regeneration, performing several functions that facilitate the healing process. After a nerve injury, Schwann cells dedifferentiate and proliferate along the remaining endoneurial tubes of the extracellular matrix (ECM), forming structures known as the bands of Büngner. These structures create a hollow tube that serves as a guided pathway for the regenerating axons to grow through (Burnett and Zager, 2004). In addition to physically supporting axon regrowth, Schwann cells communicate with the damaged neurons by sending retrograde signals. These signals lead to changes in the neuron's gene expression profile, specifically tuning it to promote regeneration (Hall, 1997). Furthermore, Schwann cells secrete neurite-promoting factors, including fibronectin and laminin, into the ECM. These proteins are crucial for the growth cones at the tips of regenerating axons, as they provide a surface for these cones to adhere to (Guénard et al., 1991). By adhering to the basal lamina of the endoneurial tubes, the growth cones can navigate through the pathway laid out by the Schwann cells, advancing the regeneration of the nerve towards the neuromuscular junction (NMJ). For the connection to become fully functional, the axon needs to undergo remyelination and increase in size (Menorca et al., 2015). These changes together enhance the axon's ability to transmit signals effectively. Ultimately, the regeneration process concludes with functional re-innervation, where the newly regenerated axon establishes a functional link with the end-organ, restoring its activity and communication.

The outcomes of nerve regeneration are significantly influenced by the integrity of the endoneurial tube. Axonotmesis, which affects the axons without harming the surrounding

connective tissue, provides an optimal environment for axonal regrowth due to the intact endoneurial tube. In neurotmesis injuries, where both the axons and endoneurial tubes are damaged, the formation of bands of Büngner is hindered, and there is an increase in scar tissue. This can block the growth cone, resulting in disorganized axonal growth (Geraldo and Gordon-Weeks, 2009). Furthermore, the gap length created by the injury is inversely related to the success of regeneration, with larger laps leading to less successful axonal outgrowth (Menorca et al., 2015). Successful regeneration and maturation also hinge on the condition of the NMJ. Following denervation, muscle fibers begin to atrophy as soon as three weeks after the injury, with collagen deposits forming in the endomysium and perimysium (Dahlin, 2006; Noaman et al., 2004). Therefore, even if a regenerated axon reaches its target, the end-organ must be preserved for the full functional recovery of the nerve.

Another issue that arises is that axons often fail to connect with their correct targets in the periphery (Brushart and Mesulam, 1980). This misdirection in reinnervation is more common after neurotmesis injuries (Brushart,1993). The absence of an intact endoneurium increases the likelihood of axons being misdirected, causing them to enter incorrect pathways, such as motor axons regenerating towards skin instead of muscles. In contrast, accurate reinnervation is more likely after crush injuries due to the presence of an intact endoneurium, which helps guide regenerating axons back to their original targets (Sunderland, 1968). This discrepancy in the reinnervation process can lead to the formation of inappropriate connections, thus decreasing the likelihood of achieving a full functional recovery.

Sensory Input Recovery in the Central Nervous System

For full functional recovery after an injury, it's crucial that not only the muscles become efficiently and precisely reinnervated motor axons and Ia sensory axons reinnervating muscle spindles. In addition, the central collaterals of Ia sensory afferents inside the spinal cord need to successfully re-establish connections motor neurons in the ventral horns. When these synaptic contacts fail to reconnect with their target neurons, both motor and sensory functions become impaired. Synapses from neurons expressing different synaptic markers exhibit varying outcomes. After successful muscle reinnervation, Vesicular Glutamate Transporter isoform 1 (VGLUT1) synapses, which label Ia afferent proprioceptive synapses (as well as II afferents), suffer a large and permanent depletion (Alvarez et al., 2011). The permanent loss of the VGLUT1 synapses, which convey information about muscle length and dynamics, has been shown to cause the permanent loss of the monosynaptic muscle stretch reflex (Bullinger et al., 2011).

As with nerve regeneration and muscle reinnervation, the fate of VGLUT1 synapses post-injury depends on multiple factors. Injury type significantly impacts recovery, with axonotmesis injuries permitting the eventual full restoration of VGLUT1 synapses, unlike neurotmesis injuries (Rotterman et al., 2024). The presence of an intact endoneurial tube accelerates nerve regeneration, resulting in faster muscle reinnervation, usually completing around 3 weeks post-injury (Rotterman et al., 2024). This condition supports the return of VGLUT1 synapses by 8 weeks post-injury. Conversely, in cases of neurotmesis, axon regeneration occurs more slowly, with full muscle reinnervation taking up to 8 weeks post-injury (Rotterman et al., 2024). After such injuries, VGLUT1 contacts do not fully re-establish connections with motor neurons, only

reaching about 20% of their original density (Rotterman et al., 2024). The lack of recovery of Ia afferent synapses has been related to developing with time microglia expressing CCL2 (Rotterman et al., 2024). This occurs after 14-21 days of continuous microglia activation and was shown to contribute to the permanent deletion of Ia afferent synapses. In contrast, microglia revert to a normal surveying microglia in none activated state after nerve crush injuries and this facilitates the return of Ia afferent synapses on motor neurons.

Another less understood factor that influences the fate of VGLUT1 synapses after injury is the age at which the injury occurs. Evidence suggests that injuries sustained during specific developmental windows impact the possibility of VGLUT1 synaptic restoration. As mentioned earlier, adults experiencing axonotmesis injuries can expect the eventual return of VGLUT1 synapses. However, when the entire nerve is transected, these synapses do not recover (Rotterman et al., 2024). In neonatal rodents of postnatal day 1 (P1) to P5, all nerve injuries regardless of modality induce the death of almost all sensory and motor neurons (Lowrie and Vrbová, 1992; Hart et al., 2008) and motor function is abolished. Lesions at early postnatal development times (around 10 days after birth in mice homologous to babies in the first 6 months of age) preserve sensory and motor neuron viability but result in lasting impairments in motor function even in the case of milder axonotmesis (crush nerves): muscle tension only recovers to half of its normal capacity, with fast-twitch muscles being more severely affected than slow-twitch ones (Lowrie et al., 1987). Additionally, the maximal compound muscle action potential (CMAP) recorded from these muscles fails to return to pre-injury levels, even 60 days post-injury, despite muscle reinnervation (Arbat-Plana et al., 2023). Moreover, Ia synapses are permanently lost over motor neuron even in the case of milder nerve injuries (Arbat-Plana et al.,

2023). The reason why axonotmesis results in more severe synapse loss in younger animals remains unclear.

The Critical Window of Developmental Synapse Pruning

The time frame during which axonotmesis leads to the permanent loss of Ia afferent/VGLUT1 synaptic contacts aligns with a crucial period of synaptic plasticity. This period is essential for the development of weight-bearing motor functions, mirroring the maturation of posture and limb coordination seen in human infants aged 8 to 15 months (Altman and Sudarshan, 1975; Westerga and Gramsbergen, 1990; Greensmith and Vrbová, 1992; Altman and Bayer, 2001). For the development of these motor functions, developmental synapse pruning must occur. This is general process that occurs during maturation of synaptic circuits throughout the central nervous system, and microglia play a pivotal role by activating genes involved in eliminating unnecessary synapses and axons (Matcovitch-Natan et al., 2016; Hammond et al., 2019, 2021). They achieve this through a mechanism known as the classical complement cascade (Stephan et al., 2012). This cascade begins with the protein C1q, which "tags" for removal synapses deemed functionally inappropriate. C1q and the complement cascade have not only been implicated in synapse pruning during development but also in the synapse pruning observed in neurodegenerative diseases such as Huntington's and Alzheimer's. Studies in mice have demonstrated the importance of complement mediated Ia afferent synapse removal during removal. The connections between Ia afferents and motor neurons are characterized by high specificity: Ia afferents from a given muscle contact motor neurons that innervate the same muscle and some synergists (motor neurons innervating muscles with similar function), but not

motor neurons that innervate antagonist (muscle with opposite function around a joint, for example flexor vs extensor). In mice lacking C1q, approximately 22% of motor neurons in the ventral horn receive inappropriate Ia afferent sensory inputs from antagonistic muscles, an error not present in wild-type mice (Vukojicic et al., 2019). This highlights the essential role of C1q and the classical complement cascade in sculpting sensory-motor circuits during early development.

The expression of genes associated with synapse and axon pruning, coupled with the observation of a permanent loss of Ia afferent synapses after axonotmesis—a loss that is less severe in adults—leads to the focus of the current study. We aim to determine whether C1q plays a different role in the synapse pruning process in young animals compared to adults, whose microglia do not upregulate pruning-associated genes in their basal state. Our study focused on analyzing Ia-motoneuron synapses in mice after a nerve crush injury at P12, comparing the outcomes between C1q-deficient animals and their control littermates. While muscle reinnervation and survival of Ia afferent neurons were similar in both groups, the loss of Ia afferent synapses did not occur in the absence of C1q. Furthermore, in adults, the extent of Ia afferent synapse loss following neurotmesis injuries was comparable in individuals with and without C1q. This indicates that while C1q is responsible for pruning these synapses in young animals, it does not contribute to the synaptic stripping observed following nerve injury in adults.

MATERIALS AND METHODS

Transgenic Models and Experimental Groups

All aspects of animal care, including surgical operations, were conducted at either Columbia University or Emory University. These procedures adhered to the National Institutes of Health Guidelines on the Care and Use of Animals and received approval from the Institutional Animal Care and Use Committee (IACUC). Several transgenic lines were obtained from The Jackson Laboratory and maintained on a C57BLk/6 background (see Table 1). Surgery procedures were conducted at either Columbia University by Dr. Danny Florez-Paz in the lab of Dr. George Mentis (Motor Center, Columbia University) or at Emory University by Ms. Zoë Haley-Johnson in the Alvarez lab. The harvested tissues were mailed to Emory University for processing and analyses.

The adult mouse group was composed of both Cx3cr1 $^{CreER/+}$ :: C1q $^{flx/flx}$ (n=3) and Cx3cr1 $^{+/+}$ :: C1q $^{flx/flx}$ mice (n=3), all of which were littermates matched in terms of age (~1.5 months old, postnatal day 46, P46) and subjected to the same injury: mid-thigh sciatic nerve transection followed by ligation preventing regeneration. Cx3cr1 $^{CreER/+}$ :: C1q $^{flx/flx}$ mice enable the induction of microglia-specific and temporally controlled C1q gene deletion. In this process, tamoxifen can be administered at a chosen time to selectively remove the *c1q* coding gene from microglia. Once tamoxifen is injected, the microglia in these mice stop producing the C1q protein required to carry out the classical complement cascade. This is a conditional *c1q* gene deletion. The Cx3cr1 $^{+/+}$ C1q $^{flx/flx}$ mice functioned as the genetic control group. This control group possesses the wild-type Cx3cr1 locus, ensuring that the C1q gene in their microglia is not

subject to tamoxifen-induced deletion. As a result, the C1q protein within the microglia in these mice remains unaltered, thereby maintaining the integrity of the classical complement pathway.

The postnatal group consisted of C1q $^{-/-}$ global knockout (KO) mice (n=5) and wild-type mice (n=4). All C1q $^{-/-}$ mice, and one wild type, were raised and nerve injured in the Mentis Lab. In this case we performed sciatic nerve crush injuries allowing regeneration to occur. Three additional mice were born at Emory, and all their surgeries and tissue processing were completed at Emory. The reason for these different sources was post-surgery death (n=1), failure to retrogradely label the sciatic motor pool (n=1) and incomplete nerve injuries (n=2) in the wild-type cohort form the Mentis lab.

In contrast to the Cx3cr1 $^{CreER/+}$ :: C1q $^{flx/flx}$ mice, the C1q $^{-/-}$ mice do not need a tamoxifen injection for the removal of the *c1q* gene. Further, the deletion of the *c1q* gene in these mice is not targeted to a specific cell type but occurs globally. This genetic alteration is present from gestation and persists throughout their lives.

In both experimental cohorts we used males and females but at present the number of animals analyzed is too small to reliably test for sex differences. This will be performed as more animals (currently under preparation) are added to the experiments.

Table 1. Mouse Models

Mouse	Jax #	Background	Donating laboratory	Reference

CX3CR1^{CreER}	020940	C57BL/6J	Dr. George Mentis, Columbia University	Yona et al., 2013
C1q $^{flx/flx}$	031261	C57BL/6N	Dr. George Mentis, Columbia University	Fonseca et al., 2017
Global C1q $^{-/-}$	031675	C57BL/6	Dr. George Mentis, Columbia University	Botto et al., 1998
Wild Type	000664	C57BL/6J	Dr. Francisco Alvarez, Emory University	Paigen et al., 1985

Tamoxifen Treatment and PNI Procedures

In mice possessing the Cx3cr1^{CreER} alleles crossed with the C1q $^{flx/flx}$ line, Cre recombinase was activated 24 hours before nerve injuries. To achieve this, 2 mg of tamoxifen, at a concentration of 5 mg/mL dissolved in peanut oil, was injected directly into the peritoneal cavity (IP). This injection triggers Cre recombination in all Cx3cr1-expressing cells, including resident microglia and certain peripheral immune cells. Effective removal of C1q was confirmed with immunohistochemistry (see below).

The adult cohort, which included both conditional microglia- *c1q* deleted mice and their control littermates, underwent sciatic nerve cut ligation surgeries. Before the injury was induced, the mice were anesthetized with isoflurane to achieve a deep surgical level of anesthesia (induction at 4–5%; maintenance at 1–3%, both in 100% O_2). An incision (~1.5 cm) was created through the skin and underlying connective tissue and the biceps femoris muscles in the mid-thigh of the right hind limb were carefully separated to expose the sciatic nerve. The nerve, once exposed, was cut with surgery scissors. To inhibit nerve regeneration, a small piece of sterile silk

was tied around the nerve's proximal stump. Following the transection and ligation of the nerve, the injury site was flushed with 0.9% sterile saline. The skin incision was then closed using absorbable sutures.

Postnatal C1q global KO animals and their wild type counterparts received sciatic nerve crush surgeries at postnatal day 12 (P12). Anesthesia and sciatic nerve exposure were performed as described above. The sciatic nerve was then crushed for 30 seconds using blunt forceps coated with Fast Blue crystals. This technique allows Fast Blue to be taken up by the nerve and retrogradely transported to the motor neurons, thereby marking the pool of injured motor neurons. The success of each crush injury was verified by ensuring that the nerve turned translucent at the crush site yet remained intact. The animals were then euthanized for collecting tissues at P30 or 18 days postsurgery. This time point was used because we expected complete muscle reinnervation by motor axons at this time point, as confirmed in the results.

After undergoing nerve injury surgeries, all animals were administered buprenorphine (subcutaneously, 0.1 mg/kg) immediately, and then every 12 hours for 48 hours as a prophylactic measure to alleviate any potential pain and distress. Mice were monitored for signs of pain or distress, such as lethargy, vocalizations, weight loss, or lack of grooming, but none were observed in any of the animals.

Harvesting Tissue for Histological Analysis

All adult animals survived for 2 weeks following nerve injury to study synaptic depletions at their peak without nerve regeneration (Rotterman et al., 2019, 2024). Postnatal

animals survived for 18 days post-injury to analyze synaptic depletion that are preserved after muscle reinnervation by motor axons is completed. The animals were deeply anesthetized using an overdose of Euthasol (100 mg/kg), and then transcardially perfused with fixatives for tissue preservation. The perfusion process began with a vascular rinse that contained heparin, effectively clearing the blood vessels. Subsequently, the tissues were infused with 4% paraformaldehyde (PFA) in 0.1 M phosphate buffer (PB) at a pH of 7.4. This procedure ensured thorough fixation of the tissues.

For the adult group comprising conditional C1q KO animals and their control littermates, only the spinal cords were extracted for subsequent analysis. All spinal cords were removed and post-fixed in a solution containing 4% PFA in 0.1 M of PB at 4°C overnight. They were then transferred to a solution containing 30% sucrose in PBS. Tissues remained in this solution until they were subjected to histological sectioning and immunohistochemistry.

The postnatalatal group, consisting of C1q global KO animals and their wild-type counterparts, received a more comprehensive dissection of different tissues. This included the extraction of the spinal cord, the left and right dorsal root ganglia (DRGs) from segments L4 and L5, along with the left and right lateral gastrocnemius (LG) and tibialis anterior (TA) muscles. The procedure for extracting and preserving the spinal cord remained consistent between these tissues and the spinal cord tissues analyzed as part of the adult cohort.

To extract the muscles, the mice were clipped at the ankle and above the knee. While the muscles remained attached to the bone, they were transferred to a 4% paraformaldehyde (PFA) solution, where they remained for 24 hours. Over the next 72 hours, the muscles were

sequentially submerged for 24 hours each in solutions of 10% sucrose, then 20% sucrose, and finally 30% sucrose.

Histological Processing and Immunohistochemistry

Spinal cords lumbar segments 4 and 5 (L4-L5) were sectioned into 50 μm thick slices using a freezing sliding microtome. The resulting slices were then processed for immunohistochemistry as free-floating sections. For all adult animals, spinal cord sections were equally divided into two vials. All sections in the vials were washed in 0.01 M PBS containing 0.3% Triton X-100 (PBS-T) and then blocked for 1 hour with 10% normal donkey serum in PBS-T. They were then incubated for approximately 24 hours at room temperature with gentle agitation in different primary antibody mixtures.

To investigate whether C1q is involved in pruning synapses after nerve injury, vial 1 was incubated in a primary antibody mixture containing guinea pig anti-VGLUT1, goat anti-choline acetyltranferase (Chat) to detect cholinergic neurons including motor neurons, and rabbit anti-Cyclic AMP-dependent transcription factor ATF3 to detect injured motor neurons. To ensure that C1q had successfully been removed from microglia, the second vial contained a mixture of chicken anti-Ionized calcium adaptor molecule 1 (Iba1) to detect microglia, rabbit anti-C1q, and mouse anti-neuronal nucleus (NeuN). Species-specific secondary antibodies conjugated to FITC, Cy3, or Cy5 were used to reveal immunoreactivities. Finally, after a last round of PBS washes, the sections were mounted with Vectashield (Vector Laboratories, Burlingame, CA, US).

Postnatal spinal cords were processed using methods similar to those for the adult cords, though they received a different primary antibody mixture. This combination, like the one in vial 1 of the adult cords, was selected to explore C1q's involvement in synaptic pruning post nerve injury. The incubation included primary antibodies for NeuN, Chat, and VGLUT1 (all the same as above). Additionally, wild type postnatal cords were stained with Iba1, VGLUT1, and C1q to investigate how microglia release C1q and interact with VGLUT1-IR synapses. In this case injured motor pools were retrogradely labeled by Fast Blue.

The DRGs and muscles from these animals were processed cut in a cryostat and processed on gals slides . The DRGs and muscles were immediately frozen in Tissue-Tek® OCT Compound (Sakura Finetek, Torrance, CA, USA). Cryostat sections of the muscles, 60 µm in thickness, were prepared and mounted on Fisherbrand Superfrost Plus slides (Fisher Scientific, Pittsburgh, PA, USA). The DRGs were sectioned at a thickness of 40 µm. These slides were then kept at 20°C until they were needed for immunohistochemistry. For labeling, the slides were first brought to room temperature and the OCT was removed with three PBS washes. The sections were blocked using 10% normal donkey serum in PBS with 0.3% Triton X-100 (PBS-T) for an hour.

To investigate the fate of the cell bodies of the Ia afferent fibers after injury, DRGs were incubated overnight with chicken anti-Parvalbumin and mouse anti-NeuN to investigate possible loss of sensory neurons because cell death. The muscles were immunostained to enable visualization of reinnervation of neuromuscular junctions (NMJs) by motor axons. For this purpose, NMJs were revealed by incubating the sections with with Alexa Fluor 647-conjugated α-bungarotoxin (α-btx, 1:100, Invitrogen, Carlsbad, CA, US) and a mix of primary antibodies.

This mix included guinea pig anti-vesicular acetylcholine transporter (VAChT) to label the motor-end plate (the synapses from motor axons) and chicken anti-neurofilament heavy chain phosphorylated (NFH) to label the motor axons. The following day, all slides were again washed in PBS and incubated for 2 hours at room temperature with secondary antibodies that were matched to the primary antibodies used. Similar to the spinal cord sections, the sections were mounted with Vectashield after a last round of PBS washes. A summary of antibody sources and catalog numbers appears in Table 2.

Table 2. Antibodies Used for Immunohistochemistry

Antigen	Immunogen	Host/type	Manufacturer	Dilution
VGLUT1	Recombinant protein (aa 456 to 560 from rat VGLUT1)	Guinea pig/polyclonal	Synaptic Systems catalog #135304	1:1000
NeuN	Purified cell nuclei from mouse brain	Mouse/monoclonal A60 clone	EMD Millipore catalog #MAB377	1:1000
Iba1	Synthetic peptide corresponding to residues near the carboxy terminus of rat IBA1	Chicken/ monoclonal recombinant IgY	Synaptic Systems catalog #234009	1:500
ATF3	Recombinant protein corresponding to amino acids (MMLQ...EKTEC)	Mouse/ monoclonal	Novus Biologicals catalog #CL1685	1:100
Chat	Human placental enzyme	Goat/polyclonal	EMD Millipore catalog #AB144P	1:100

C1q	Full length native protein corresponding to mouse C1q	Rabbit/ monoclonal	Abcam catalog #82451	1:1000
NFH	Native NF-H purified from bovine spinal cord.	Chicken/ polyclonal	Encor catalog #CPCA-NF-H	1:1000
VAChT	Recombinant protein corresponding to residues near the carboxy terminus of rat VAChT	Guinea pig/ polyclonal	Synaptic Systems catalog #139105	1:500

Analysis of VGLUT1 Densities on 3D Reconstructed MNs

The spinal cord sections from both adults and postnatal mices, containing labeled LG MNs and VGLUT1-IR synapses, were imaged using an Olympus FV1000 confocal microscope. Imaging was performed at both low magnification (10x, z-step: 1.5 μm, NA 0.4) and high magnification (60x, z-step: 1 μm). All sections were imaged on both injured and uninjured sides using identical parameters. High magnification images were uploaded to Neurolucida 360 for the partial reconstruction of motor neuron surfaces. This involved tracing the neuron across 13 confocal mid-plane optical planes. Mid-plane optical sections of the cell body were identified by the presence of the nucleolus. VGLUT1 synaptic contacts on all motor neuron optical cross-sections were then counted based on specific criteria: the synapse must be in contact with the motor neuron surface and visible in at least two optical planes, but only counted once.

Subsequently, these reconstructions were imported into Neurolucida Explorer for analysis of the cell body surface. The surface area analyzed was estimated by calculating the total surface of the partially reconstructed cell body object and then subtracting the areas contributed by the cut surfaces. For each animal, 20 motor neuron cell bodies were reconstructed: 10 from the injured side and 10 from the uninjured side. This resulted in the partial reconstruction and quantification of 120 motor neurons from the adult animals and 200 from the postnatal group.

Analysis of VGLUT1 Contact Size

To assess the size of VGLUT1-IR contacts upon motor neurons, neurons exhibiting VGLUT1-IR soma densities closest to the average for each respective animal and injury status were selected across all conditions. The optical plane in which the synapse of interest appeared in-focus, and the corresponding image was imported into ImageJ. There, a region of interest (ROI) was delineated around the synapse. Next, all channels except for the one displaying VGLUT1-IR in black and white were eliminated. The image was then subjected to thresholding to generate a 2D mask of the synapse, and the area of this reconstruction was recorded.

Due to the varying densities of VGLUT1 between each condition, the quantified number of synapses also differed accordingly, with conditions exhibiting lower VGLUT1 densities resulting in fewer synapses quantified. To maintain data consistency, we utilized these individual synapse size quantifications and determined the average per animal per condition for further analysis

Quantifying Muscle Reinnervation

Images of TA and LG muscle tissue were acquired at 20x magnification with a z-step size of 1µm. These images were then transferred to Neurolucida 360 for manual quantification of dual-labeled structures. Neuromuscular junctions (NMJs) positive for both α-btx and VAChT were identified as innervated. Conversely, NMJs marked solely by α-btx, in the absence of VAChT staining, were classified as not reinnervated.

Muscle samples were collected from six neonatal animals. Of these, three were from animals with global C1q KOs, and the remaining three were from their corresponding genetic controls. For each animal, between 120 and 240 NMJs were analyzed, with the number of NMJs evaluated per condition (injured or uninjured) ranging from 60 to 120. Overall, approximately 250 NMJs were quantified for each condition across all animals.

To quantify the extent of reinnervation, the number of reinnervated NMJs was determined for each animal and condition (injured or uninjured), and then expressed as a percentage of the total NMJs evaluated within that specific animal and condition. This process allowed us to calculate the percent reinnervation for both the injured and uninjured sides of each animal. Subsequently, data from individual animals were aggregated to derive an estimate of the overall percent reinnervation within each condition, for both the TA and LG muscles.

Statistical Comparisons of VGLUT1 Synaptic Density

The data was first organized in Prism (GrahPad) for a Nested-ANOVA analysis taking into account animal and repetitive measures from individual motor neurons and using four

experimental groups: Wild-type control and injured side, conditional (adult) or global KO (neonate) control and injured side. These analyses resulted in significance for the adult nerve transection experiment, but not for the P12 nerve crush experiment due to high interanimal variability. Thus, we conducted one-way ANOVAs across animals within each animal cohort and this resulted in detection of interanimal variability in all experimental cohorts in the P13 experiment, but not within the animals in the adult experimental groups (Table 2). Therefore, we proceeded to analyze the data by comparing the experimental side to the control side using paired t-tests and estimating of effect sizes by calculating the mean difference and the 95% confidence limits of this difference. Because adult animals 14 days after nerve transection showed no variability, we were able to group their data and perform a two-way ANOVA for genetics (wild type vs conditional microglia C1q KO and spinal cord side (experimental vs control).

Table 3. Interanimal Variability in Different Experimental Groups for VGLUT1 Density (one-way ANOVAs)

Experimental group	N (animal), n (motoneurons)	F value	Degrees of freedom	P value
Adult P45				
Wild Type Control	3	1.500	2	0.2418
Wild Type Experimental	3	1.870	2	0.1736
Conditional KO Control	3	1.079	2	0.3540
Conditional KO Experimental	3	1.303	2	0.2883

Neonatal P12				
Wild Type Control	4	14.19	3	<0.0001****
Wild Type Experimental	4	5.313	3	0.0039**
Global KO Control	5	2.743	4	0.0399*
Global KO Experimental	5	9.948	4	<0.0001****

Statistical Comparisons of VGLUT1 Synapses Sizes

Statistical analyses that evaluated VGLUT1 synapse size differences were also done using Prism (GraphPad) . The data was organized as before. In neonates, due to non-normal distribution and interanimal variability, initial analyses used Kruskal-Wallis one-way ANOVAs to evaluate interanimel variability in the different groups. When this was rejected, we pooled all animals within each group and compared their average sizes. The distribution of VGLUT1 average sizes followed normality allowing using a two-way ANOVA to assess the effects of injury status and genotype. Paired t-tests analyzed within-animal synapse size changes, offering insights into injury impacts. For adults, with no significant interanimal variability, two-way ANOVAs directly assessed genotype and injury status effects, with paired t-tests for within-animal comparisons.

Table 4. Interanimal Variability in Different Experimental Groups for Synapse Size

Experimental group	N (animal), n (motoneurons)	F value	Degrees of freedom	P value

Adult P45				
Wild Type Control	3	1.808	2	0.2832
Wild Type Experimental	3	N/A	N/A	0.2185
Conditional KO Control	3	N/A	N/A	0.5013
Conditional KO Experimental	3	0.5508	2	0.5508
Neonatal P12				
Wild Type Control	4	2.104	4	0.0903ns
Wild Type Experimental	4	N/A	N/A	0.0001***
Global KO Control	5	N/A	N/A	0.0407*
Global KO Experimental	5	N/A	N/A	0.2967ns

RESULTS

To explore the involvement of C1q in the elimination of VGLUT1-IR synapses following a sciatic nerve crush injury during the postnatal period, we utilized mice of two genotypes: those with a global deletion of C1q and their wild-type counterparts of the same age who experienced the same injury. C1q initiates the classical pathway of the complement cascade; thus, in its absence, this pathway cannot proceed. Each group of mice underwent a sciatic nerve crush injury at postnatal day 12 (P12), a critical phase during which after axotomy of the sensory axons in the peripheral nerve the cell bodies of proprioceptors are spared, yet their synapses on motor neurons (MNs), marked by VGLUT1-IR, are known to go through significant developmental plasticity dependent on microglia and C1q mechanisms. We therefore tested whether an injury, even mild like nerve crush, will induce synapses losses larger than normal.

C1q is necessary for VGLUT1 synaptic losses after nerve crush injury in neonates

To identify MNs injured in the nerve, these were retrogradely labeled with Fast Blue at the time of injury by applying Fast Blue crystals while crushing the sciatic nerve (Fig. 1A1). We examined the loss of VGLUT1 boutons specifically around the retrogradely labeled MNs 18 days post-injury, that is at P30 (Fig. 1A2). In these animals we also visualized IBA1-positive microglia (Fig. 1A3) and C1q immunoreactivity (Fig. 1A4). According to prior studies in young rats, peak microgliosis is observed 7 days after a sciatic nerve crush injury (Arbat-Plana et al., 2023), suggesting that at our chosen time point, microgliosis would be near its basal level. However, given the active upregulation of C1q at this stage to facilitate developmental synapse pruning, an increase in C1q expression within microglia can be observed, but mainly in the dorsal horn (Fig. 1A4). Nevertheless, even at 18 days post-injury, microglia carrying C1q were seen surrounding motor neurons and extending their processes towards VGLUT1-IR synapses (Fig. 1B). Furthermore, C1q puncta were observed in proximity to, or "tagging," VGLUT1-IR synapses (Fig. 1C1-C3).

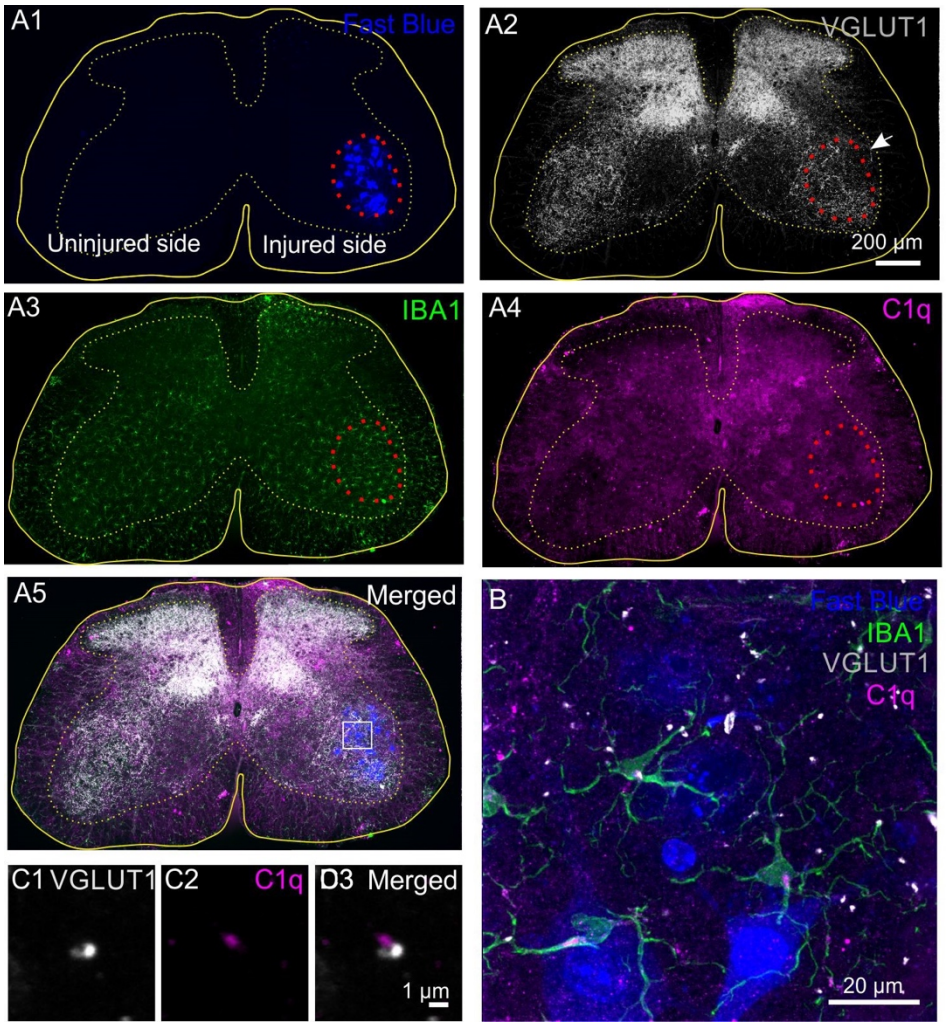

Figure 1. VGLUT1-IR synapse loss, microglia reaction and C1q 18 days after P12 sciatic nerve crush.

Panels (A1-5) display z-stack projections from confocal image stacks through a 50 µm thick section, revealing four fluorescent signals analyzed: Fast Blue MNs (A1), VGLUT1-immunoreactive (IR) synaptic boutons (A2), IBA1 microglia (A3), and C1q (A4). A composite image of all signals is also shown (A5). Red dotted lines denote the injured motor neurons. The white arrow in panel (A2) highlights the sciatic motor pool region where we can see a reduction in VGLUT1-IR puncta on the side ipsilateral to the nerve injury. The solid yellow line marks the spinal cord boundary, while the dotted line delineates the gray matter. The white square in (A5) highlights the approximate location of the lateral gastrocnemius (LG) motor pool area. Panel (B) shows the highlighted LG area at higher magnification, featuring z-stack images of Fast Blue,

IBA1, and C1q, along with a single optical plane of VGLUT1. Panel (C1-3) illustrates a VGLUT1-IR bouton in proximity to a C1q punctum.

To investigate the role of C1q in the removal of VGLUT1 synapses we labeled some sections for CHAT, VGLUT1 and NeuN (Fig. 2A1-5) and quantified VGLUT1 synapses on the cell bodies of sciatic MNs across four conditions: (1) uninjured motor neurons in animals expressing C1q (Fig. 2B1), (2) injured motor neurons in animals expressing C1q (Fig. 2C1), (3) uninjured motor neurons in animals with a global C1q knockout (KO) (Fig. 2D1), and (4) injured motor neurons in animals with a C1q KO (Fig. 2E1). Injured motorneurons were labeled with fast blue, CHAT, and NeuN, while uninjured motorneurons were labeled by only CHAT and NeuN. Both CHAT and NeuN are known to decrease after axotomy, but their normal intensity in the injured sited in these images is indirect evidence that these MNs have reinnervated muscle. To estimate the density of the VGLUT1 contacts upon the MNs, we created partial 3D reconstructions of the cell body surface of MNs using Neurolucida (Fig. 2B2, 2C2, 2D2, 2E2) (see also methods).

The density of VGLUT1 synapses per 100 μm^2 motor neurons was determined, categorized by genotype, injury status, and individual animal (Fig. 2F1). We first compared interanimal variability within each experimental group. After confirming that the data from each animal (10 MN cell bodies) was normally distributed we performed within group one-way ANOVAS and found significant animal variability (Table 2). Given the substantial inter-animal variability observed, including discrepancies among MNs under identical conditions, it was inappropriate to pool the data for a Nested or 2-way ANOVA. This variability might have come by technical differences in the preparation of different samples (fixation, immunohistochemistry, ... etc). Therefore, we performed within animal comparisons (Fig. 2F2). We calculated the average

VGLUT1 density for each animal and condition, and subsequently conducted two-tailed paired t-tests comparing only injury vs uninjured side in wild-types and C1q global KOs.

This analysis revealed that VGLUT1 synaptic density on injured motor neurons in wild-type animals consistently decreased (Fig. 2F2). Conversely, C1q global KO mice did not exhibit a discernible pattern (Fig. 2F3). Specifically, we observed a 55% decrease in VGLUT1 synaptic density, with a standard deviation of ±11%, between the uninjured and injured sides of wild-type animals, and no significant decrease between the uninjured and injured MNs in the C1q KO animals. This indicates a significant reduction in VGLUT1 synapses upon injury in the presence of C1q, but not in its absence. These findings imply that C1q plays a crucial role in the elimination of VGLUT1 synapses following peripheral nerve crush injuries during early postnatal development.

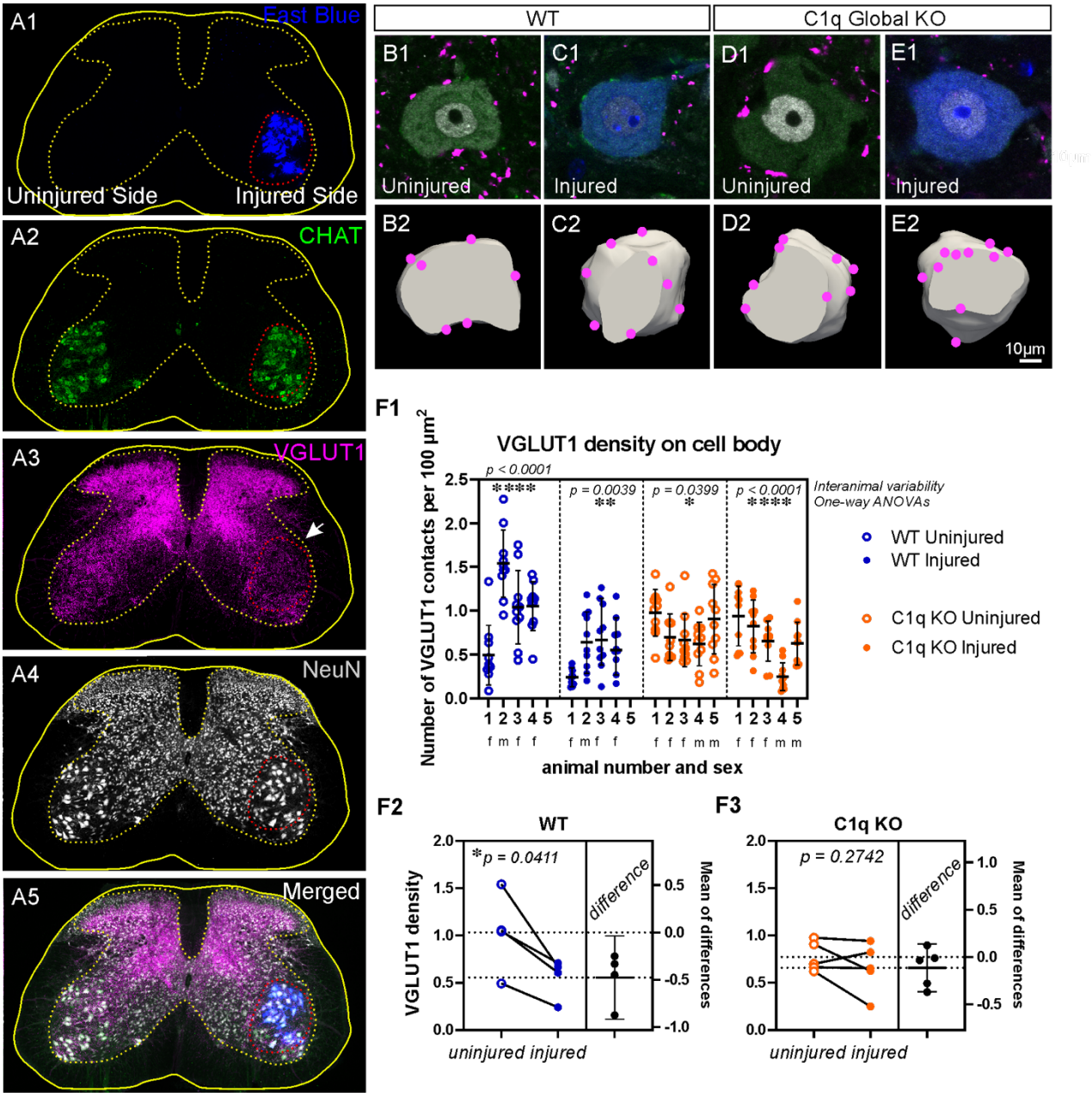

Figure 2. Preservation of VGLUT1-IR synapses following nerve crush injury in postnatal mice lacking C1q

Panels (A1-A5) display confocal z-stack 2D projections of a 50 µm-thick sections of the spinal cord 18 days post-sciatic nerve crush injury: Fast Blue-labeled motor neurons (MN) (A1), CHAT-positive motor neurons (A2), VGLUT1-immunoreactive synaptic boutons (A3), NeuN-mature neurons (A4), and a composite image integrating all markers (A5). Anatomical landmarks are

delineated: the spinal cord boundary with a solid yellow line, the gray matter with a yellow dotted line, and the injured motor neuron pool area with a red dotted line. The sciatic motor pool region, on the side ipsilateral to the injury, shows a marked decrease in VGLUT1-immunoreactive puncta (pointed out with a white arrow), suggesting synaptic depletion (A3). High-magnification, single-plane images of MNs separated by condition (B1, C1, D1, E1). Beneath these, 3D reconstructions of partial MN surfaces, with magenta circles indicating VGLUT1 synaptic contacts. Panel (F1) shows estimated VGLUT1 densities in all MNs sampled in each animal and experimental group. Each MN is one dot. Horizontal lines are the mean and error bars S.D. Each animal number and sex indicated in the x-axis (f: female, m: male). One-way ANOVAs show large interanimal variability. Panels (F2) and (F3) show estimation plots from paired t-tests comparing mean differences between the uninjured and uninjured side in each animal for wild-types (WTs) (F2) and C1q global KOs (F3). A significant difference was found in WTs but not in C1q global KOs (all p values are indicated).

The size of preserved synapses decreases in both WTs and C1q global KOs

To evaluate the functionality of VGLUT1 synapses, we measured the sizes of synaptic boutons on motor neurons, based on the premise that larger boutons from Ia afferents indicate stronger synaptic connections, while smaller synapses correspond to weaker inputs (Pierce and Mendell, 1993; Pierce and Lewin, 1994).

We analyzed synaptic bouton areas at midpoint confocal planes, sorting the data by genotype, injury status, and individual animals (Fig. 3B1-B4). When the data sets were tested for normality, we found that the data distribution for synapse sizes often deviated from normality. This is likely a result of confocal microscopy resolution limitations: the smaller synaptic boutons could not be resolved such that datasets are skewed towards larger synapses because a cut-off limit measuring smaller synapses. Therefore, data sets were compared for interanimal variability using Kruskal-Wallis one-way ANOVAs and we must assume that the size of smaller synapses might be overestimated in all samples. We observed only limited variability in synapse sizes across

animals: in the WT injured side animal #4 was smaller than three other and in the uninjured side of C1q global KOs animals #4 and #5 revealed a small difference (Fig. 3C1). We calculated an average for each animal. Animal averages were normally distributed permitting the use of parametric statistical tests. A two-way ANOVA showed a significant effect of injury status ($p < 0.0001$), but not of C1q genotype ($p = 0.1379$), with a significant interaction between these factors ($p = 0.0386$) (Fig. 4C2, left). This suggests that, on average, synapses on MNs following regeneration after P12 injuries are of smaller size. This result was confirmed using paired t-tests for within animal comparisons (Fig. 3C2, right). These findings suggest that synapse size and therefore VGLUT1 synaptic functionality was similarly decreased on MNs of WTs and C1q-absent animals after injury. The results highlight the injury's impact on synaptic integrity independent of C1q presence. We did not calculate a percentage size decrease because of the expected overestimation of small synapse sizes.

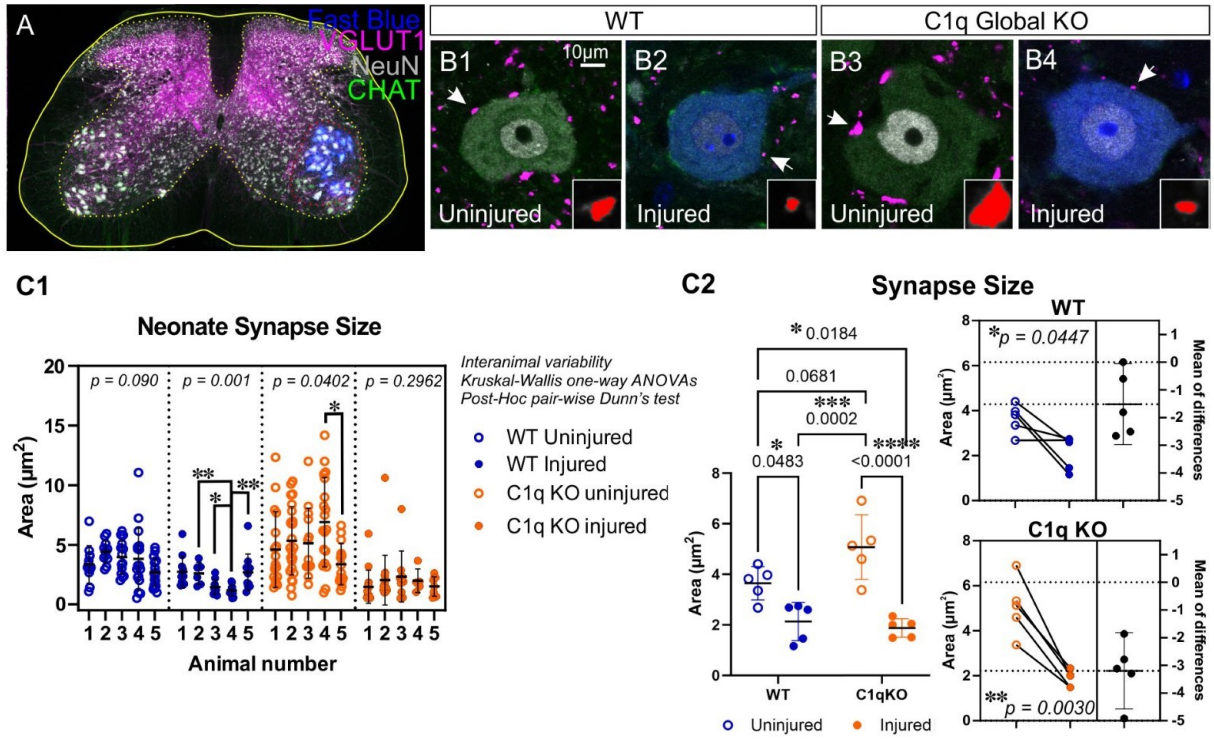

Figure 3. Neonate synapse size after injury in wild-types and C1q global KOs

Panels (A) display a confocal z-stack 2D projection from through a 50 µm thick section, revealing distinct fluorescent markers in the spinal cord 18 days post-sciatic nerve crush injury: Fast Blue-labeled MNs, CHAT-positive motor neurons, VGLUT1 synaptic boutons, NeuN-expressing mature neurons. Anatomical landmarks are delineated: the spinal cord boundary with a solid yellow line, the gray matter with a yellow dotted line, and the injured motor neuron pool area with a red dotted line. Panels (B1-B4) are high-magnification, single-plane images of individual MNs separated by condition. On the bottom right of each image is an enlarged, thresholded view of the quantified synapse indicated by a white arrow. (C1) illustrates synapse size estimations across different conditions, using brackets and asterisks to denote significant differences in synapse sizes within the same condition. Panel (C2, left graph), two-way ANOVA analysis based on the average synapse area per animal. Statistical significances are indicated. Panel (C2, right graphs), within animal paired t-tests and estimation differences for Wild-types (WTs) and C1q global KOs all tests indicate that synapses on MNs after injury (and regeneration) are significantly smaller independent on whether is in C1q wild -types or C1q global KOs.

At the end point used in the study (18 days post-injury) muscle reinnervation is similar and complete, independent of C1q presence.

To exclude the possibility that VGLUT1 alterations was a consequence of different rates of regeneration and muscles reinnervation in the absence of C1q we examined the reinnervation of neuromuscular junctions (NMJs) in the lateral gastrocnemius (LG) and tibialis anterior (TA) muscles. We labeled NMJs with Alexa-555 conjugated a-bungarotoxin. This toxin binds strongly to nicotinic cholinergic receptors labeling the postsynaptic NMJ region. We also used antibodies against the vesicular acetylcholine transporter (VACHT) to label the motor endplate (the MN synapse) and antibodies against phosphorylated neurofilament heavy chain (NFH) to label the motor axons. NMJs were considered reinnervated if opposed by a VAChT motor endplate emerging from a motor axon (Fig 4).

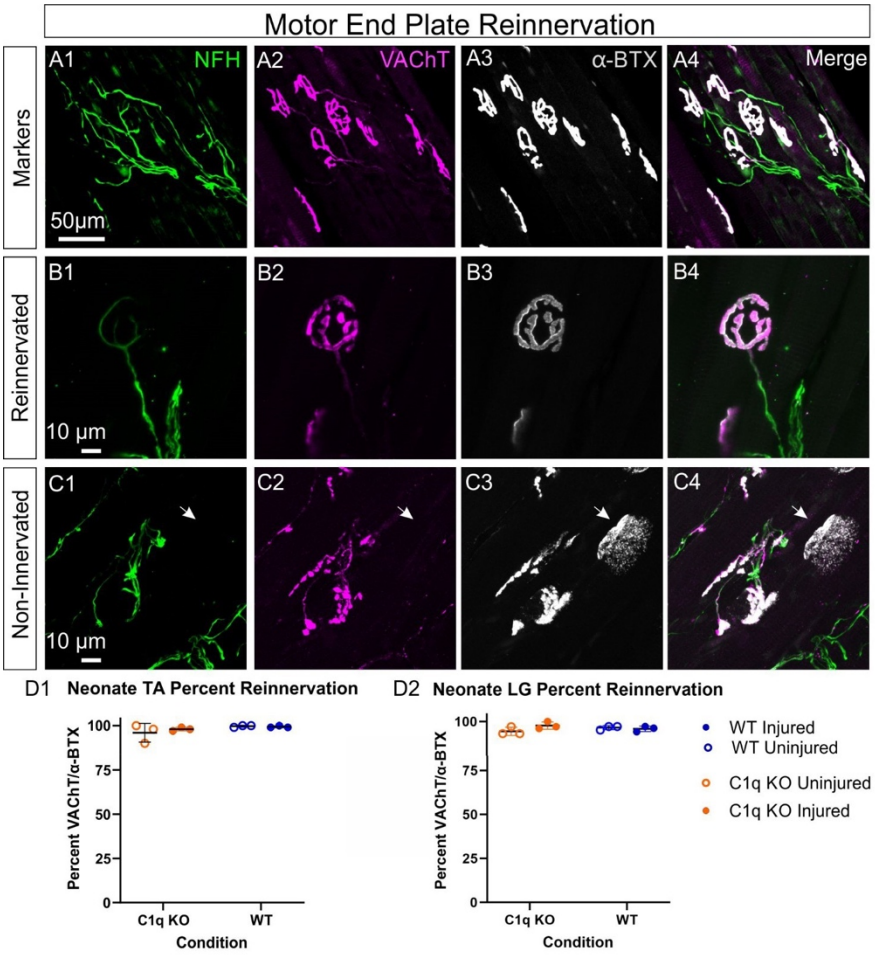

Figure 4. Reinnervation of motor end plates in wild-types and C1q global KOs

Panels A1-A4 feature z-stack projections of confocal image stacks through a 60 μm thick section of muscle tissue, illustrating three fluorescent markers: (A1) NFH-labeled motor axons, (A2) VAChT-positive motor end-plates, (A3) α-BTX-labeled neuromuscular junctions (NMJs), and (A4) a composite image showing all fluorescent signals merged. Panels B1-B4 highlight a reinnervated NMJ, demonstrating dual labeling with VAChT and α-BTX, and its connection to motor axons. Panels C1-C4 depict one non-reinnervated NMJ (white arrow). Panels D1-D2 show the percentage of reinnervated NMJs across all conditions. Two-way ANOVA followed by Tukey multiple comparisons showed no significant differences.

We examined around 50 NMJs in 3-4 high magnification images in each muscle and animal (n =3). In the LG and TA muscles at least 90% reinnervated, a threshold which constitutes full

functional recovery (Rotterman et al., 2024). A two-way ANOVA for injury and C1q deletion followed by post-hoc pair-wise Tukey tests found no significant differences in NMJ innervation among animals in either the TA or LG, yet a small significant difference among animal according to C1q genetics was revealed by the ANOVA in the LG ($p=0.0216^*$), although no significance was found in post-hoc Tukey tests. We conclude that any small differences in reinnervation of the LG 18 days postinjury in the condition of C1q global KO is very small. New animals are currently being investigated to confirm or falsify this result.

In summary, our findings indicate complete reinnervation of both TA and LG muscles 18 days post-injury across all animals injured at P12, irrespective of their genotype: C1q KO or WT. Consequently, the reduction in VGLUT1-positive synaptic boutons or their sizes cannot be attributed to lack of MN reinnervation of muscle.

Microglia express and release C1q after nerve injury in adult spinal cords.

In early postnatal mice, C1q is actively upregulated in microglia as part of the developmental synaptic pruning process (Matcovitch-Natan et al., 2016; Hammond et al., 2019, 2021). In contrast, adult microglia do not express C1q in their basal state. Nonetheless, C1q has been implicated in synaptic pruning during neurodegenerative diseases in adults (reviewed in Stephan et al., 2012). To explore whether C1q is upregulated after peripheral nerve injury in adults, and whether all C1q is derived from activated microglia, we localized C1q by immunolabeling after sciatic nerve transections before and after conditionally knocking out the *c1q* gene specifically from microglia 24 hours before sciatic nerve transections. For analyses we chose 14 days after injury, a timepoint associated with peak microglial response around the injured motor

neurons (Rotterman et al., 2024). In this experiment we labeled the sections for IBA1 microglia, C1q and NeuN. At this time point MNs have not reinnervated muscle targets and NeuN therefore stays depleted following downregulation induced by the axotomy. This gives a convenient marker to identify injured motor pools (Fig.5A1-5).

In mice with intact C1q expression, microglia and C1q cluster around injured MNs (Fig. 5A1-5, Fig. 5C2). The immunohistochemical analysis confirmed that microglia are the primary source of C1q as demonstrated by complete absence of C1q immunoreactivity following its knockout in microglia (Fig. 5B2). This confirms a previous study that used *c1q* mRNA in situ hybridization methods to detect the sources of C1q in the spinal cord after nerve injury (Berg et al., 2012). Despite the absence of C1q, microglia continued to accumulate (Fig. 5B1) in the area containing injured MNs (Fig. 5B3).

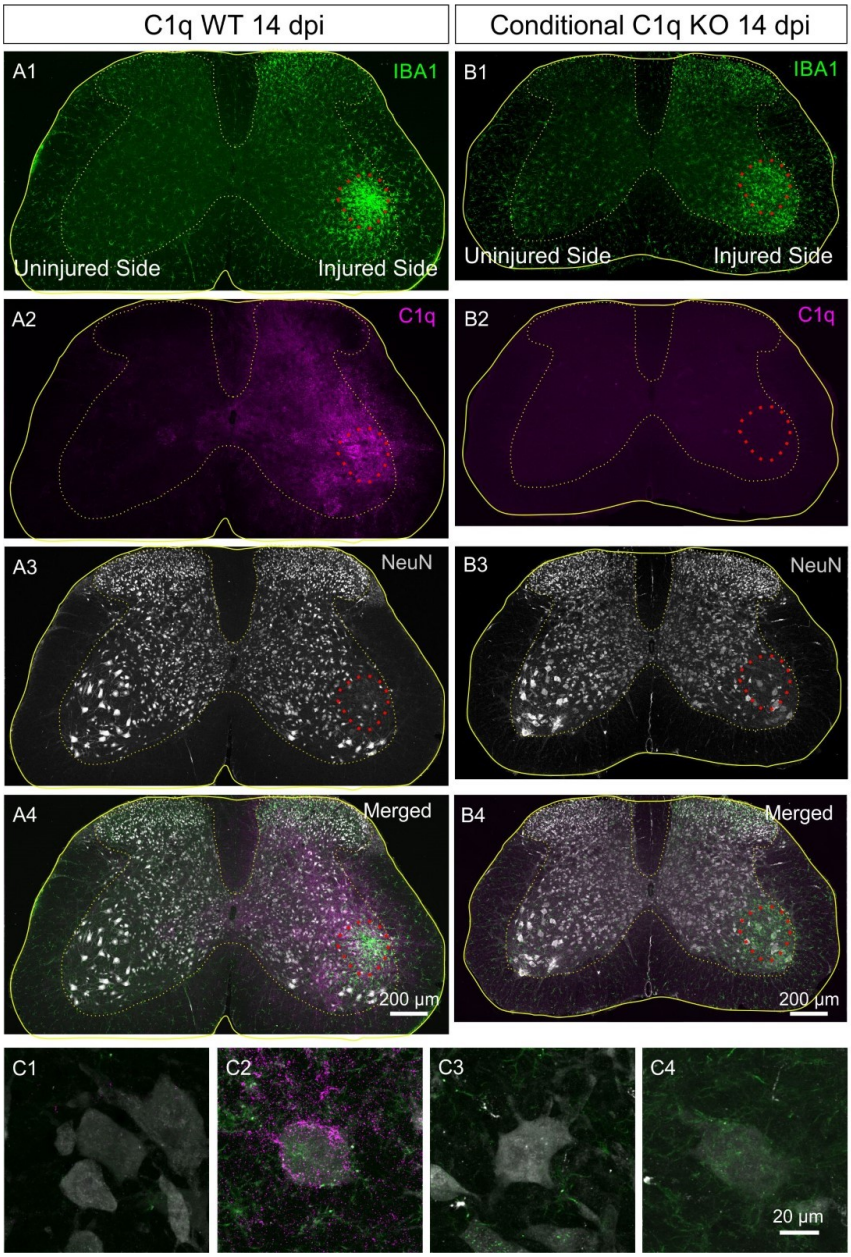

Figure 5. Successful depletion of C1q from microglia in adult conditional C1q KO mice

(A1-4 and B1-4) z-stack 2D projections of confocal stacks through 50 µm thick sections from a wild-type (A1-4) and an animal in which C1q was conditionally removed from microglia (B1-4) 14 days after unilateral sciatic nerve transection. They show the three fluorescent signals analyzed: IBA1 *microglia (A1, B1), C1q (A2, B2), NeuN (A3, B3), and a merge of all channels (A4, B4). Solid yellow lines indicate the spinal cord edge. Dotted lines mark the gray matter. The dotted red lines locate injured motor pools (NeuN negative). (C1-4) high magnification images of*

MNs from a wild-type (C1-2) and an animal with C1q deleted from microglia (C3-4), showing uninjured (C1, C3), and injured MNs (C2, C4).

C1q is not necessary for VGLUT1 synapse plasticity 14 days after nerve transection in adults

After establishing that C1q is released from activated microglia and associates with MN cell body surfaces following injury, we aimed to determine if removing C1q would preserve VGLUT1 synapses in adults as it does in neonates. Serial sections from the animals described in the previous section were labeled with CHAT to define MN cell bdoy surfaces (NeuN is downregulated), ATF3 to identify axotomized MNs and VGLUT1 (Fig. 6 A1-4). Injured MNs were identified by CHAT and ATF3 in the nucleus (Fig. 6B1, D1), and uninjured MNs by CHAT only (Fig. 6C1, E1). Like our approach with neonates, we created 3D reconstructions of MN cell body surfaces to assess VGLUT1 contact density (Fig. 6B2, C2, D2, E2).

Our analysis revealed that all the data followed normal distributions with no interanimal variability (Table 2), enabling the use of a nested one-way ANOVA followed by post-hoc Tukey tests for multiple comparisons. Our findings included significant differences between injured and uninjured states in both wild-types ($p = 0.0008$***) ($p = 0.0056$**) and C1q microglia KOs. No significant differences in VGLUT1 density were observed between C1q microglia KO injured and WT injured MNs ($p=0.9645$), or between C1q KO uninjured and WT uninjured MNs ($p = 0.2028$ (Fig. 7F1). Subsequently, we conducted paired t-tests comparing injured and uninjured motor neurons within both genotypes. This analysis revealed a significant reduction of 47% (±5.5 SD) in VGLUT1 contacts between uninjured and injured WT MNs ($p=0.0073$**) (Fig. 7F2). Similarly, a significant decrease of 54% (±11 SD) in VGLUT1 contacts was observed between uninjured and

injured C1q microglia KO MNs (p=0.0322*) (Fig. 6F3). These findings suggest that C1q is not essential for the elimination of VGLUT1 synapses in adult mice.

To further explore the functionality of synapses as we did with neonates, we assessed the sizes of the VGLUT1 contacts. Bouton sizes data sets showed no interanimal variability (tested with Kruska-Wallis ANOVAs because similar data in neonates' size distributions were not normally distributed) (Fig. 7C1). This prevented the use of a Nested ANOVA and led us to perform a two-way ANOVA using the animal averages (which we confirmed were normally distributed). This analysis revealed no significant differences according to genotype (p=0.0930), injury status (p=0.2025), or the interaction between these two variables (p=0.2160) (Fig. 8C2, left graph). This conclusion was confirmed by "within animals" comparisons using paired t-test (Fig. 7C2, right graph).

These findings indicate that injury decreases VGLUT1 synapse numbers on MNs, but do not affect their size—and by extension, their function. However, previous studies reported that remaining synapses fail to recover stretch reflexes (Rotterman et al., 2024) and a trend towards smaller sizes was observed. Because only 3 animals were studied in each condition this statistical comparison might be underpowered and we are currently preparing more animals

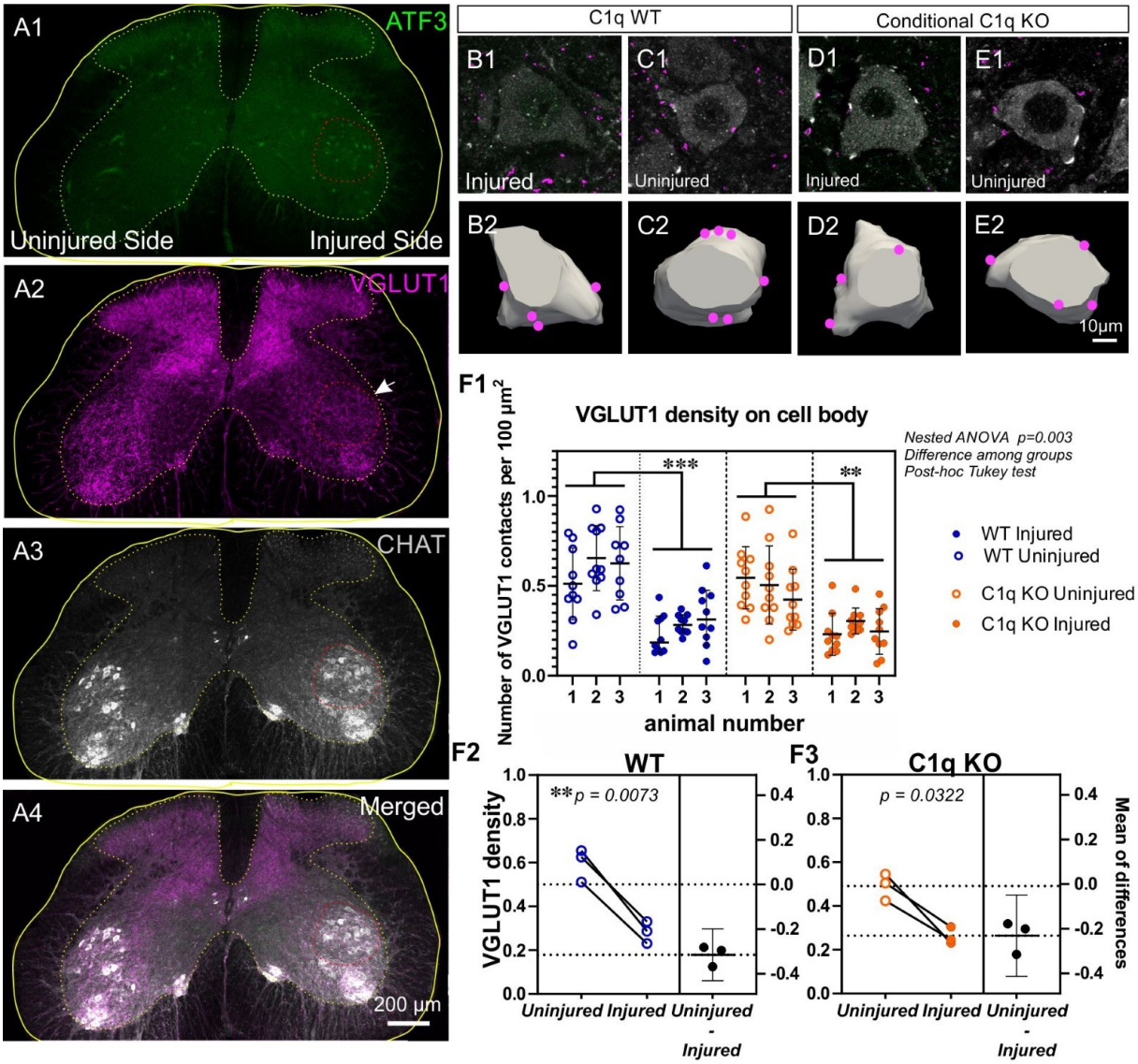

Figure 6. Lack of preservation of VGLUT1-IR synapses after nerve cut injury in C1q conditional KO adult mice

Panels (A1-A5) present confocal z-stack projections form 50 µm thick sections of the spinal cord, captured 14 days after a sciatic nerve cut ligation injury. These images reveal the distinct fluorescent markers used : ATF3 upregulation in the nuclei of injured motor neurons (MNs) (A1), VGLUT1 synaptic boutons (A2), CHAT-positive MNs (A3), and a composite image that integrates all markers (A4). Anatomical landmarks within the spinal cord define the boundary of the spinal cord (solid yellow line), the gray matter (yellow dotted line), and the area of the injured motor neuron pool (dotted red line). Notably, within the sciatic motor pool region, which is ipsilateral to the injury, there is a significant reduction in VGLUT1-IR puncta, as highlighted by a white arrow in (A2), indicating synaptic depletion. Panels (B1, C1, D1, E1) feature high-magnification, single-

*plane images of quantified MNs, categorized by condition. Below these images, 3D reconstructions illustrate partis reconstructions of MN cell body surfaces and magenta circles mark VGLUT1 synaptic contacts. Panel (F1) quantifies the VGLUT1 contacts per 100 µm² of motor neuron surface area, with the data organized by animal number, genotype, and injury status. Each MN is one dot. Horizontal lines are the mean and error bars S.D. Each animal number is indicated in the x-axis. A nested one-way ANOVA followed by post-hoc Tukey tests show significant differences between injury and non-injury side in both wild-types and animals with conditional removal of C1q form microglia (**p<0.01, ***p<0.001). Furthermore, panels (F2) and (F3) display estimation plots from paired t-tests that compare the mean differences in VGLUT1 contacts between uninjured and injured MNs in individual WT and C1q conditional knockouts (KO) animals. VGLUT1 synapses are significantly depended in both situations.*

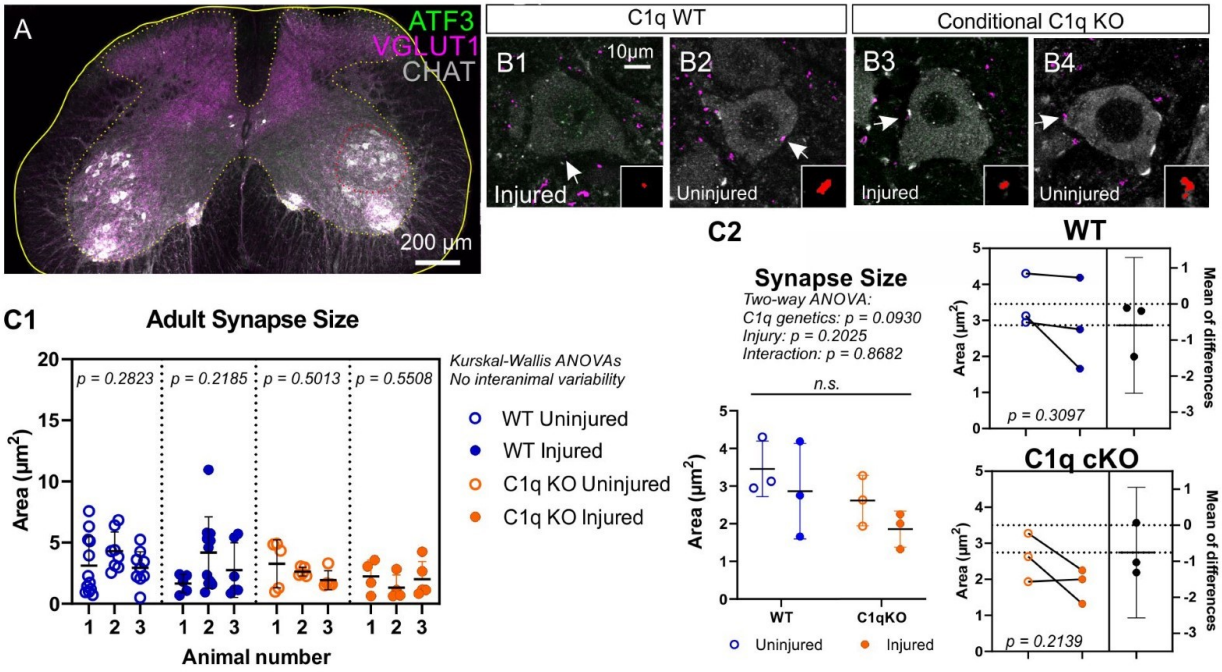

Figure 7. Adult synapse size is unaffected by injury or presence of C1q.

Panel A displays a confocal z-stack projection through a 50 µm thick section of the spinal cord, taken 14 days post-sciatic nerve cut ligation injury showing superimposed ATF3 upregulation in injured MNs, VGLUT1 synaptic boutons, and CHAT-positive MNs. Landmarks within the spinal cord are delineated a s in previous figures. Panels B1-B4 show high-magnification, single-plane images of individual MNs, categorized by condition. The bottom right corner of each image shown an enlarged and thresholded synapse (marked with a white arrow). Panel C1 shows synapse size estimations across different conditions, showing no interanimal variability within experimental

groups. Panel C2 (graph at left) shows a two-way ANOVA analysis of average synapse sizes per animal. The result showed no statistical differences detected. Panel C2 (graph at right) confirms this result using paired –tests in within animal analyses.

DISCUSSION

In this study, we delve into the mechanisms of synaptic pruning following peripheral nerve injuries, with a focus on the role of C1q and the complement cascade during the early postnatal period. This phase is marked by significant synaptic plasticity, making it an interesting time for studying the effects of nerve crush injuries. Such injuries during this period lead to the significant and permanent losses of VGLUT1 synaptic contacts, critical for transmitting sensory information from muscle spindle proprioceptors to spinal α-motoneurons. This permanent loss occurs despite the full reinnervation of muscles (Arbat-Plana et al., 2023). Here, we investigate why these synapses are permanently lost, and whether C1q, known for its role in synaptic elimination during developmental stages and pathological conditions (Stephan et al., 2012), plays a part in this process.

Given the active upregulation of C1q by microglia during this period, we hypothesized that C1q is implicated in the injury-induced synaptic pruning observed. Our findings suggest that C1q is indeed necessary for the permanent removal of Ia afferent synapses observed post-injury in neonates. This aligns with the broader understanding of C1q's role in developmental synaptic pruning and adds a novel perspective on its role in injury-induced synaptic changes.

When comparing the neonatal injury model to adult nerve crush models, we observed similar synaptic losses but through seemingly different mechanisms (Rotterman et al., 2019; 2024). In the absence of C1q, neonatal VGLUT1 boutons remained, whereas in adults lacking C1q, these synapses were still lost. This difference suggests a novel role of C1q in injury-induced neonatal synaptic pruning and suggests alternative mechanisms are at play in adults, potentially involving CCR2-CCL2 signaling mechanisms and the infiltration of peripheral immune cells following nerve transection as recently proposed (Rotterman et al., 2019; 2024). These findings suggest that milder nerve injuries are more deleterious in neonates than adults, inducing more plasticity in motor synaptic circuitry in the spinal cord.

To indirectly assess the functionality of the remaining synapses, we estimated their functionality through immunohistochemistry, focusing on synaptic bouton size as a proxy for synaptic strength. Larger boutons are indicative of stronger synaptic connections (Pierce and Mendell, 1993; Pierce and Lewin, 1994). Our results indicate that post-nerve transection in adults, the remaining synapses are larger and therefore likely more functional than those in neonates, irrespective of C1q presence. Nevertheless, in these mice Ia afferent input cannot recruit motor neurons to fire after muscle stretch and the stretch reflex still does not recover following regeneration after nerve transection (Rotterman et al., 2024). However, after nerve crush in the adult the stretch reflex recovers and in fact is enhanced.

In contrast, boutons remain very small following regeneration after nerve crush in neonates. This finding coupled with evidence that muscle tension only recovers to half its normal capacity post-reinnervation in the early postnatal period (Lowrie et al., 1987; Kemp et al., 2015), suggests a large functional deficit after nerve crush in neonates. Comparison of synaptic bouton

sizes in animals with C1q present or depleted were no different and this further suggests that while C1q is involved in synaptic removal in neonates, an alternative mechanism likely contributes to the functional silencing of these synapses.

Future Directions

Future investigations should aim to further elucidate C1q's role in VGLUT1 synaptic dynamics post-PNI. One potential future study may involve conditional C1q knockout models in neonates. This could help to differentiate between developmental synaptic pruning and injury-induced pruning.

Additionally, to gain a better understanding of the functionality of the VGLUT1 synapses after injury, future studies can measure H-responses. H-responses tests evaluate the sensory and motor pathway function by activating the monosynaptic muscle stretch reflex. Conducting this tests offers a measure of the physiological impact of synaptic losses or preservation, and how this may differ between C1q and injury statuses.

Much work is yet to be done to understand how C1q is involved in synaptic plasticity after nerve injury in adults. Although our study indicates that C1q is not necessary for VGLUT1 synapse removal in adults, it may still play a supplementary role in synaptic pruning post-injury. We observed that C1q accumulates around motor neurons following injury (Fig. 5C2), yet its specific role here is yet to be understood. We also need to analyze time points after 14 days in which regeneration has been completed to evaluate whether C1q is still not relevant for delayed synaptic losses after 14 days.

In conclusion, our study supports the notion that complement-mediated synaptic removal, plays a critical role in the loss of Ia afferent synapses following early postnatal nerve crush injuries. However, the functionality of the remaining synapses appears compromised, suggesting that C1q's role in synaptic pruning during development differs significantly from its role in adult nerve injuries. Further research into the mechanisms of synaptic pruning and recovery post-PNI will be important for improving functional recovery after peripheral nerve injuries.

REFERENCES

Althagafi, A., & Nadi, M. (2023, August 7). Acute nerve injury. In StatPearls. StatPearls Publishing. Retrieved from https://www.ncbi.nlm.nih.gov/books/NBK549848/

Altman, J., & Bayer, S. A. (2001). Development of the human spinal cord: An interpretation based on experimental studies in animals. Oxford University Press, USA.

Altman, J., & Sudarshan, K. (1975). Postnatal development of locomotion in the laboratory rat. Animal behaviour, 23(4), 896–920. https://doi.org/10.1016/0003-3472(75)90114-1

Alvarez, F. J., Titus-Mitchell, H. E., Bullinger, K. L., Kraszpulski, M., Nardelli, P., & Cope, T. C. (2011). Permanent central synaptic disconnection of proprioceptors after nerve injury and regeneration. I. Loss of VGLUT1/IA synapses on motoneurons. Journal of neurophysiology, 106(5), 2450–2470. https://doi.org/10.1152/jn.01095.2010

Arbat-Plana, A., Bolívar, S., Navarro, X., Udina, E., & Alvarez, F. J. (2023). Massive loss of proprioceptive Ia synapses in rat spinal motoneurons after nerve crush injuries in the postnatal period. eNeuro, 10(2), ENEURO.0436-22.2023. https://doi.org/10.1523/ENEURO.0436-22.2023

Bähr, M., & Przyrembel, C. (1995). Myelin from peripheral and central nervous system is a nonpermissive substrate for retinal ganglion cell axons. Experimental neurology, 134(1), 87–93. https://doi.org/10.1006/exnr.1995.1039

Berg, A., Zelano, J., Stephan, A., Thams, S., Barres, B. A., Pekny, M., Pekna, M., & Cullheim, S. (2012). Reduced removal of synaptic terminals from axotomized spinal motoneurons

in the absence of complement C3. Experimental neurology, 237(1), 8–17. https://doi.org/10.1016/j.expneurol.2012.06.008

Botto, M., Dell'Agnola, C., Bygrave, A. E., Thompson, E. M., Cook, H. T., Petry, F., Loos, M., Pandolfi, P. P., & Walport, M. J. (1998). Homozygous C1q deficiency causes glomerulonephritis associated with multiple apoptotic bodies. *Nature genetics*, *19*(1), 56–59. https://doi.org/10.1038/ng0598-56

Brushart, T. M., & Mesulam, M. M. (1980). Transganglionic demonstration of central sensory projections from skin and muscle with HRP-lectin conjugates. Neuroscience letters, 17(1-2), 1–6. https://doi.org/10.1016/0304-3940(80)90051-8

Bullinger, K. L., Nardelli, P., Pinter, M. J., Alvarez, F. J., & Cope, T. C. (2011). Permanent central synaptic disconnection of proprioceptors after nerve injury and regeneration. II. Loss of functional connectivity with motoneurons. Journal of neurophysiology, 106(5), 2471–2485. https://doi.org/10.1152/jn.01097.2010

Burnett, M. G., & Zager, E. L. (2004). Pathophysiology of peripheral nerve injury: A brief review. Neurosurgical focus, 16(5), E1. https://doi.org/10.3171/foc.2004.16.5.2

Carroll, S. L., & Frohnert, P. W. (1998). Expression of JE (monocyte chemoattractant protein-1) is induced by sciatic axotomy in wild type rodents but not in C57BL/Wld(s) mice. Journal of neuropathology and experimental neurology, 57(10), 915–930. https://doi.org/10.1097/00005072-199810000-00004

Dahlin, L. B. (2006). Nerve injury and repair: From molecule to man. In Slutsky DJ, Hentz VR (Eds.), Peripheral Nerve Surgery: Practical Applications in the Upper Extremity.

Dong, S., Feng, S., Chen, Y., Chen, M., Yang, Y., Zhang, J., Li, H., Li, X., Ji, L., Yang, X., Hao, Y., Chen, J., & Wo, Y. (2021). Nerve suture combined with ADSCs injection under real-time and dynamic NIR-II fluorescence imaging in peripheral nerve regeneration in vivo. Frontiers in chemistry, 9, 676928. ttps://doi.org/10.3389/fchem.2021.676928

Duffy, B. J., & Tubog, T. D. (2017). The prevention and recognition of ulnar nerve and brachial plexus injuries. Journal of perianesthesia nursing: Official journal of the American Society of PeriAnesthesia Nurses, 32(6), 636–649.

https://doi.org/10.1016/j.jopan.2016.06.005

Ertürk, A., Hellal, F., Enes, J., & Bradke, F. (2007). Disorganized microtubules underlie the formation of retraction bulbs and the failure of axonal regeneration. The Journal of neuroscience: The official journal of the Society for Neuroscience, 27(34), 9169–9180.

https://doi.org/10.1523/JNEUROSCI.0612-07.2007

Fonseca, M. I., Chu, S. H., Hernandez, M. X., Fang, M. J., Modarresi, L., Selvan, P., MacGregor, G. R.,& Tenner, A. J. (2017). Cell-specific deletion of C1qa identifies microglia as the dominant source of C1q in mouse brain. *Journal of neuroinflammation*, *14*(1), 48.

https://doi.org/10.1186/s12974-017-0814-9

Fu, S. Y., & Gordon, T. (1997). The cellular and molecular basis of peripheral nerve regeneration. Molecular neurobiology, 14(1-2), 67–116. https://doi.org/10.1007/BF02740621

George, R., & Griffin, J. W. (1994). Delayed macrophage responses and myelin clearance during Wallerian degeneration in the central nervous system: The dorsal radiculotomy model. Experimental neurology, 129(2), 225–236. https://doi.org/10.1006/exnr.1994.1164

Geraldo, S., & Gordon-Weeks, P. R. (2009). Cytoskeletal dynamics in growth-cone steering. Journal of cell science, 122(Pt 20), 3595–3604. https://doi.org/10.1242/jcs.042309

Gilliatt, R. W., & Hjorth, R. J. (1972). Nerve conduction during Wallerian degeneration in the baboon. Journal of neurology, neurosurgery, and psychiatry, 35(3), 335–341. https://doi.org/10.1136/jnnp.35.3.335

Goodman, C. S. (1996). Mechanisms and molecules that control growth cone guidance. Annual review of neuroscience, 19, 341–377. https://doi.org/10.1146/annurev.ne.19.030196.002013

Govindan, M., & Burrows, H. L. (2019). Neonatal brachial plexus injury. Pediatric reviews, 40(9), 494-496. https://doi.org/10.1542/pir.2018-0113

Greensmith, L., & Vrbová, G. (1992). Alterations of nerve-muscle interaction during postnatal development influence motoneurone survival in rats. Brain research. Developmental brain research, 69(1), 125–131. https://doi.org/10.1016/0165-3806(92)90129-k

Guénard, V., Dinarello, C. A., Weston, P. J., & Aebischer, P. (1991). Peripheral nerve regeneration is impeded by interleukin-1 receptor antagonist released from a polymeric guidance channel. Journal of neuroscience research, 29(3), 396–400. https://doi.org/10.1002/jnr.490290315

Hall, S. (1997). Axonal regeneration through acellular muscle grafts. Journal of anatomy, 190(Pt 1), 57–71. https://doi.org/10.1046/j.1469-7580.1997.19010057.x

Hammond, B. P., Manek, R., Kerr, B. J., Macauley, M. S., & Plemel, J. R. (2021). Regulation of microglia population dynamics throughout development, health, and disease. Glia, 69(12), 2771-2797.

Hammond, T. R., Dufort, C., Dissing-Olesen, L., Giera, S., Young, A., Wysoker, A., Walker, A. J., Gergits, F., Segel, M., Nemesh, J., Marsh, S. E., Saunders, A., Macosko, E., Ginhoux, F., Chen, J., Franklin, R. J. M., Piao, X., McCarroll, S. A., & Stevens, B. (2019). Single-cell RNA sequencing of microglia throughout the mouse lifespan and in the injured brain reveals complex cell-state changes. Immunity, 50(1), 253–271.e6. https://doi.org/10.1016/j.immuni.2018.11.004

Hart, A. M., Terenghi, G., & Wiberg, M. (2008). Neuronal death after peripheral nerve injury and experimental strategies for neuroprotection. Neurological research, 30(10), 999–1011. https://doi.org/10.1179/174313208X362479

Lleva, J. M. C., Munakomi, S., & Chang, K. V. (2023). Ulnar neuropathy. In StatPearls

[Internet]. Treasure Island (FL): StatPearls Publishing; 2024. Available from: https://www.ncbi.nlm.nih.gov/books/NBK534226/

Lopes, B., Sousa, P., Alvites, R., Branquinho, M., Sousa, A. C., Mendonça, C., Atayde, L. M., Luís, A. L., Varejão, A. S. P., & Maurício, A. C. (2022). Peripheral nerve injury treatments and advances: One health perspective. International journal of molecular sciences, 23(2), 918. https://doi.org/10.3390/ijms23020918

Lowrie, M. B., & Vrbová, G. (1992). Dependence of postnatal motoneurones on their targets: Review and hypothesis. Trends in neurosciences, 15(3), 80–84. https://doi.org/10.1016/0166-2236(92)90014-y

Lowrie, M. B., Krishnan, S., & Vrbová, G. (1987). Permanent changes in muscle and motoneurones induced by nerve injury during a critical period of development of the rat. Brain research, 428(1), 91–101. https://doi.org/10.1016/0165-3806(87)90086-1

Lubińska, L. (1977). Early course of Wallerian degeneration in myelinated fibres of the rat phrenic nerve. Brain research, 130(1), 47–63. https://doi.org/10.1016/0006-8993(77)90841-1

Maas, H., Prilutsky, B. I., Nichols, T. R., & Gregor, R. J. (2007). The effects of self-reinnervation of cat medial and lateral gastrocnemius muscles on hindlimb kinematics in slope walking. Experimental brain research, 181(2), 377–393.

https://doi.org/10.1007/s00221-007-0938-8

Matcovitch-Natan, O., Winter, D. R., Giladi, A., Vargas Aguilar, S., Spinrad, A., Sarrazin, S., ... & Amit, I. (2016). Microglia development follows a stepwise program to regulate brain homeostasis. Science, 353(6301), aad8670.

McKerracher, L., David, S., Jackson, D. L., Kottis, V., Dunn, R. J., & Braun, P. E. (1994). Identification of myelin-associated glycoprotein as a major myelin-derived inhibitor of neurite growth. Neuron, 13(4), 805–811. https://doi.org/10.1016/0896-6273(94)90247-x

McQuarrie, I. G. (1985). Effect of conditioning lesion on axonal sprout formation at nodes of Ranvier. The Journal of comparative neurology, 231(2), 239–249. https://doi.org/10.1002/cne.902310211

Menorca, R. M., Fussell, T. S., & Elfar, J. C. (2013). Nerve physiology: Mechanisms of injury and recovery. Hand clinics, 29(3), 317–330. https://doi.org/10.1016/j.hcl.2013.04.002

Morris, J. H., Hudson, A. R., & Weddell, G. (1972). A study of degeneration and regeneration in the divided rat sciatic nerve based on electron microscopy. II. The development of the "regenerating unit". Zeitschrift fur Zellforschung und mikroskopische Anatomie (Vienna, Austria : 1948), 124(1), 103–130.

Mukhopadhyay, G., Doherty, P., Walsh, F. S., Crocker, P. R., & Filbin, M. T. (1994). A novel role for myelin-associated glycoprotein as an inhibitor of axonal regeneration. Neuron, 13(3), 757–767. https://doi.org/10.1016/0896-6273(94)90042-6

Noaman, H. H., Shiha, A. E., & Bahm, J. (2004). Oberlin's ulnar nerve transfer to the biceps motor nerve in obstetric brachial plexus palsy: Indications, and good and bad results. Microsurgery, 24(3), 182–187. https://doi.org/10.1002/micr.20037

Paigen, B., Morrow, A., Brandon, C., Mitchell, D., & Holmes, P. (1985). Variation in susceptibility to atherosclerosis among inbred strains of mice. Atherosclerosis, 57(1), 65 73. https://doi.org/10.1016/0021-9150(85)90138-8

Pierce, J. P., & Lewin, G. R. (1994). An ultrastructural size principle. Neuroscience, 58(3), 441–446. https://doi.org/10.1016/0306-4522(94)90071-x

Pierce, J. P., & Mendell, L. M. (1993). Quantitative ultrastructure of Ia boutons in the ventral horn: scaling and positional relationships. The Journal of neuroscience: the official journal of the Society for Neuroscience, 13(11), 4748–4763.

https://doi.org/10.1523/JNEUROSCI.13-11-04748.1993

Reichert, F., Saada, A., & Rotshenker, S. (1994). Peripheral nerve injury induces Schwann cells to express two macrophage phenotypes: Phagocytosis and the galactose-specific lectin MAC-2. The Journal of neuroscience: The official journal of the Society for

Neuroscience, 14(5 Pt 2), 3231–3245.

https://doi.org/10.1523/JNEUROSCI.14-05-03231.1994

Rotshenker, S. (2011). Wallerian degeneration: The innate-immune response to traumatic nerve injury. Journal of neuroinflammation, 8, 109. https://doi.org/10.1186/1742-2094-8-109

Schäfer, M., Fruttiger, M., Montag, D., Schachner, M., & Martini, R. (1996). Disruption of the gene for the myelin-associated glycoprotein improves axonal regrowth along myelin in C57BL/Wlds mice. Neuron, 16(6), 1107–1113. https://doi.org/10.1016/s0896-6273(00)80137-3

Shamash, S., Reichert, F., & Rotshenker, S. (2002). The cytokine network of Wallerian degeneration: Tumor necrosis factor-alpha, interleukin-1alpha, and interleukin-1beta. The Journal of neuroscience: The official journal of the Society for Neuroscience, 22(8), 3052–3060. https://doi.org/10.1523/JNEUROSCI.22-08-03052.2002

Stephan, A. H., Barres, B. A., & Stevens, B. (2012). The complement system: an unexpected role in synaptic pruning during development and disease. Annual review of neuroscience, 35, 369–389. https://doi.org/10.1146/annurev-neuro-061010-113810

Stoll, G., Griffin, J. W., Li, C. Y., & Trapp, B. D. (1989). Wallerian degeneration in the peripheral nervous system: Participation of both Schwann cells and macrophages in myelin degradation. Journal of neurocytology, 18(5), 671–683. https://doi.org/10.1007/BF01187086

Subang, M. C., & Richardson, P. M. (2001). Influence of injury and cytokines on synthesis of monocyte chemoattractant protein-1 mRNA in peripheral nervous tissue. The European journal of neuroscience, 13(3), 521–528. https://doi.org/10.1046/j.1460-9568.2001.01425.x

Sunderland, S. (1951). A classification of peripheral nerve injuries producing loss of function. Brain: a journal of neurology, 74(4), 491–516. https://doi.org/10.1093/brain/74.4.491.

Sunderland, S. (1968). Nerves and nerve injuries. Edinburgh, E & S Livingstone Ltd.

Tuttle, R., & O'Leary, D. D. (1998). Neurotrophins rapidly modulate growth cone response to the axon guidance molecule, collapsin-1. Molecular and cellular neurosciences, 11(1-2), 1–8. https://doi.org/10.1006/mcne.1998.0671

Volpe, J. J., Inder, T. E., Perlman, J. M., et al. (2018). Neurology of the Newborn. Elsevier. https://doi.org/10.1016/C2010-0-68825-0

Vukojicic, A., Delestrée, N., Fletcher, E. V., Pagiazitis, J. G., Sankaranarayanan, S., Yednock, T. A., Barres, B. A., & Mentis, G. Z. (2019). The classical complement pathway mediates microglia-dependent remodeling of spinal motor circuits during development and in SMA. Cell reports, 29(10), 3087–3100.e7. https://doi.org/10.1016/j.celrep.2019.11.013

Westerga, J., & Gramsbergen, A. (1990). The development of locomotion in the rat. Brain research. Developmental brain research, 57(2), 163–174. https://doi.org/10.1016/0165-3806(90)90042-w

Yona, S., Kim, K. W., Wolf, Y., Mildner, A., Varol, D., Breker, M., Strauss-Ayali, D., Viukov, S., Guilliams, M., Misharin, A., Hume, D. A., Perlman, H., Malissen, B., Zelzer, E., & Jung, S. (2013). Fate mapping reveals origins and dynamics of monocytes and tissue macrophages under homeostasis. *Immunity*, *38*(1), 79–91.

https://doi.org/10.1016/j.immuni.2012.12.001

Zhang, S., Huang, M., Zhi, J., Wu, S., Wang, Y., & Pei, F. (2022). Research hotspots and trends of peripheral nerve injuries based on Web of Science from 2017 to 2021: A bibliometric analysis. Frontiers in neurology, 13, 872261. https://doi.org/10.3389/fneur.2022.872261